

ANL-5544

Reactors-Research & Power

ARGONNE NATIONAL LABORATORY
P. O. Box 299
Lemont, Illinois

EXPERIMENTAL BOILING WATER REACTOR (EBWR)
SHIELD DESIGN

by

M. Grotenhuis and J. W. Butler

Reactor Engineering Division

August, 1956

Operated by The University of Chicago
under
Contract W-31-109-eng-38

DISCLAIMER

This report was prepared as an account of work sponsored by an agency of the United States Government. Neither the United States Government nor any agency Thereof, nor any of their employees, makes any warranty, express or implied, or assumes any legal liability or responsibility for the accuracy, completeness, or usefulness of any information, apparatus, product, or process disclosed, or represents that its use would not infringe privately owned rights. Reference herein to any specific commercial product, process, or service by trade name, trademark, manufacturer, or otherwise does not necessarily constitute or imply its endorsement, recommendation, or favoring by the United States Government or any agency thereof. The views and opinions of authors expressed herein do not necessarily state or reflect those of the United States Government or any agency thereof.

DISCLAIMER

Portions of this document may be illegible in electronic image products. Images are produced from the best available original document.

TABLE OF CONTENTS

	<u>Page</u>
ABSTRACT	7
I. INTRODUCTION	7
II. METHOD OF ANALYSIS	7
III. DESIGN PROCEDURE AND SPECIAL PROBLEMS	11
IV. SHIELD DESIGN CALCULATIONS.	13
A. Fast Neutron Flux	13
1. Light Water-Moderated EBWR.	13
2. Heavy Water-Moderated EBWR	14
B. Thermal Neutron Flux.	18
1. Light Water-Moderated EBWR.	18
2. Heavy Water-Moderated EBWR	25
C. Gamma-Ray Flux	25
V. HEAT GENERATION.	38
BIBLIOGRAPHY.	42

3

LIST OF FIGURES

<u>No.</u>	<u>Title</u>	<u>Page</u>
1	Arrangement for Removal Cross-Section Measurement.	8
2	Illustration for Fast Neutron Flux Calculation.	9
3	Spherical Source with Slab Shields.	13
4	Vertical Section of the Light-Water Moderated EBWR Vessel and Shield.	16
5	Calculated Fast Neutron Flux in the EBWR Shield (H ₂ O Reflector)	17
6	Vertical Section of the EBWR Vessel and Shield as Altered to Include Operation as a Heavy Water Moderated Reactor	19
7	Calculated Fast Neutron Flux in the EBWR Shield (D ₂ O Reflector)	20
8	Calculated Thermal Neutron Flux in the EBWR Radial Shield (H ₂ O Reflector).	23
9	Calculated Thermal Neutron Flux Above the EBWR Core (H ₂ O Reflector)	23
10	Calculated Axial Thermal Neutron Flux Below the EBWR Core (H ₂ O Reflector)	24
11	Calculated Thermal Neutron Flux in the EBWR Radial Shield (D ₂ O Reflector).	27
12	Calculated Thermal Neutron Flux Above the EBWR Core (D ₂ O Reflector)	28
13	Calculated Thermal Neutron Flux Below the EBWR Core (D ₂ O Reflector)	29
14	Geometry for Plane Volume Source with Slab Shields	29
15	Higher Order F Functions	31
16	Calculated Gamma-Ray Flux in the EBWR Radial Shield (H ₂ O Reflector)	34
17	Calculated Gamma-Ray Flux Above the EBWR Core (H ₂ O Reflector)	35
18	Calculated Gamma-Ray Flux Below the EBWR Core (H ₂ O Reflector)	36

LIST OF FIGURES

<u>No.</u>	<u>Title</u>	<u>Page</u>
19	Calculated Gamma-Ray Fluxes in the EBWR (D ₂ O Reflector)	37
20	Calculated Heat Generation in the EBWR Shield (H ₂ O Reflector)	40
21	Calculated Heat Generation in the EBWR (D ₂ O Reflector)	41

LIST OF TABLES

<u>No.</u>	<u>Title</u>	<u>Page</u>
I	Constants Used for the Calculation of the Fast Neutron Flux in Light Water-Moderated EBWR Shielding.	15
II	Constants Used for the Calculation of the Fast Neutron Flux in Heavy Water-Moderated EBWR Shielding.	21
III	Constants Used for the Calculation of the Thermal Neutron Flux in the Light Water-Moderated EBWR Shielding.	22
IV	Constants Used for the Calculation of the Thermal Neutron Flux in the Heavy Water-Moderated EBWR Shielding.	26
V	Gamma-Ray Absorption Coefficients (H ₂ O Reflector)	33
VI	Gamma-Ray Absorption Coefficients (D ₂ O Reflector)	38

NOMENCLATURE

B	Beam Attenuation Kernel	
D_s	Thermal Neutron Diffusion Constant	cm
J_f	Current of Fast Neutrons	$n/cm^2 \text{ sec}$
K_n	Conversion Factor	$(n/cm^2 \text{ sec})/(mrep/hr)$
K_γ	Conversion Factor	$(mr/hr)/(\gamma/cm^2 \text{ sec})$
k	Reciprocal Relaxation Length for Gamma-Ray Source Strength	cm^{-1}
N	Measured Beam Attenuation Kernel for Fission Neutrons in Water	$(mrep/hr)/(watt/cm^2)$
N_γ	Number of Gamma Rays per Neutron Capture	
n	Number of Kinds of Shield Materials	
Q_n	Fast Neutron Source Strength	$watt/cm^3$ or $n/cm^3 \text{ sec}$
Q_γ	Gamma-Ray Source Strength	$\gamma/cm^3 \text{ sec}$
R	Radius	cm
κ	Reciprocal of Thermal Neutron Diffusion Length	cm^{-1}
μ	$\cos \theta$	
ν	k/σ_s	
ρ	Optical Path Length in Water	cm
σ_s	Effective Source Removal Cross Section or Gamma-Ray Absorption Coefficient	cm^{-1}
σ_r	Fast Neutron Removal Cross Section	cm^{-1}
σ_a	Thermal Neutron Absorption Cross Section	cm^{-1}
σ	Constant Adjusted for Continuity of Fast Neutron Flux as Thermal Neutron Source Strengths or Gamma-Ray Absorption Coefficient	cm^{-1}
Φ_f	Fast Neutron Flux	$n/cm^2 \text{ sec}$
Φ_s	Thermal Neutron Flux	$n/cm^2 \text{ sec}$
Φ_γ	Gamma-Ray Flux	$\gamma/cm^2 \text{ sec}$

6

EXPERIMENTAL BOILING WATER REACTOR (EBWR) SHIELD DESIGN

by

M. Grotenhuis and J. W. Butler

ABSTRACT

The Experimental Boiling Water Reactor (EBWR) shield and the methods used in the design are described. The report includes shield adjustments necessary to make a change from light-water moderator to heavy-water moderator.

I. INTRODUCTION

The design of the EBWR shield consisted of two phases, each of which was a separate shield study. The first design^(1, 2) was for the original conception of the EBWR: a light water-moderated reactor with an ordinary concrete biological shield. The second study^(3, 4) came about when the decision was made to include the possibility of operating the same facility as a heavy water-moderated reactor. The shielding problems encountered in the second study indicated that heavy water-moderated operation would require more shielding; however, it was not economically feasible to alter the reactor vessel or the total shield thickness. The additional shielding was incorporated, therefore, by including a boron-steel thermal shield and by increasing the density of part of the concrete shield.

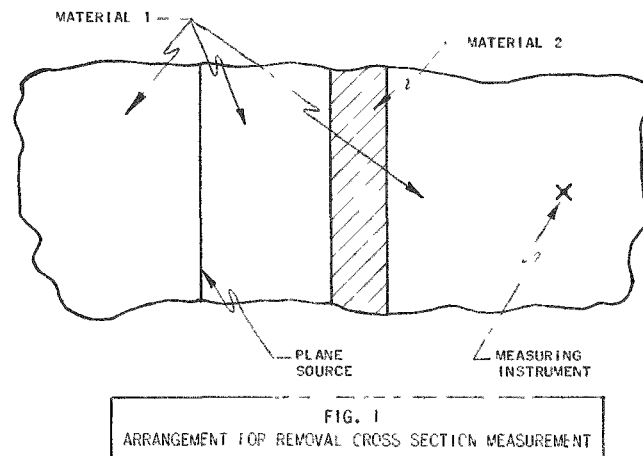
The factors leading to the required increase in shielding were a moderate increase in the fast neutron flux and a rather large increase in thermal neutron flux. These factors and their effect on the shield design will be treated in detail in the sections of this report dealing with the design calculations. Briefly, these flux increases affected the total shield design in two ways: the radiation heating in the reactor vessel and the capture gamma-ray fluxes penetrating the shield were both increased substantially.

II. METHOD OF ANALYSIS

In the practical design of a reactor shield it is necessary to first compute the emergent fast neutron dose, then the thermal neutron flux, and finally the emergent gamma-ray dose. If the total dose rate at the outer surface of the shield exceeds design specifications, it is then necessary to alter the amount and disposition of the shielding materials and to repeat the calculation.

The neutron analysis used in this report follows the "removal theory" of shield design, which was implicitly introduced by Welton and Albert^(5,6) and has since been given a firmer foundation and a somewhat different conceptual basis by the work of Blizard and other in the Oak Ridge Shielding Group. The central concept in this theory is that of the removal cross section. (7, 12, 13) This quantity can best be defined by describing an ideal experiment for measuring it.

Consider, as in Fig. 1, an infinite medium composed of material #1 in which there is a plane source of neutrons with a certain energy spectrum, usually a fission spectrum. At some distance from the source, depending on the nature of the medium and upon the energy and angular distribution of the source, the neutron distribution will have a characteristic shape which is independent of the angular distribution of the source neutrons; furthermore, this shape will be independent of the energy response of the detecting instrument used to measure it.



A slab of another material, called material #2, is now introduced into the medium, and the neutron flux in the medium of material #1 is measured at a sufficient distance from the slab so that the characteristic flux shape is again established. If the slab of material #2 is now removed, leaving the void which it occupied, the flux as measured at this same point will increase. If this experiment is repeated for a range of slab thicknesses and positions, and if it is found that the attenuation caused by the slab of material #2 can be described by an exponential function of a constant of proportionality times its thickness, this constant is then defined to be the removal cross section of material #2 with respect to material #1.

In cases in which this method is directly applicable, the neutron attenuation of the shield is accomplished principally by one dominant material, usually water or other hydrogenous material, and the effect of introducing other materials, structure, etc., is described by use of the removal cross section. The experiment described above is, of course, highly idealized, and in both measurement and application geometrical compromises are made. Thus, most removal cross sections have been measured in the Lid Tank Facility at Oak Ridge, (14) which consists of a large tank of water containing a 28-in. diameter disc source of fission neutrons. Hence, the values so obtained are removal cross sections with respect to water as the principal neutron-attenuating substance.

In order to make practical use of these numbers, some method must be introduced for dealing with geometrical configurations met in practice. This may be done by assuming that the radiation travels from source to detector along the optical path connecting them, the attenuation due to each material being apportioned according to the thickness of that material traversed by the optical path. The attenuation in the water component is calculated by making use of the measured attenuation for that thickness of water; the attenuation in the other components is taken into account by use of removal cross sections as described above. Once the principle of straight-ray propagation has been accepted, the radiation from sources of complex shape surrounded by appropriate shield configurations can be calculated by integration of contributions from different parts of the source. While this is simple in principle, very complicated integral expressions may result unless the geometry is simplified as much as possible. In a general situation, such as in Fig. 2,

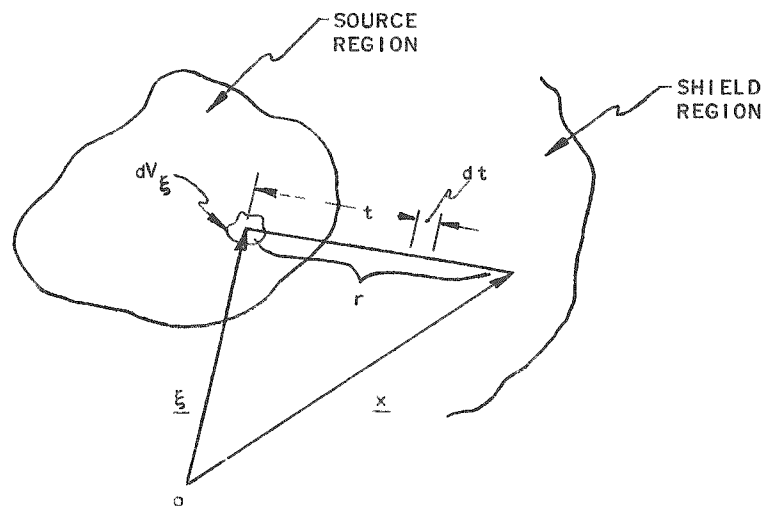


FIG. 2
ILLUSTRATION FOR FAST NEUTRON FLUX CALCULATION

the fast flux is given by

$$\Phi_f(\underline{x}) = \int_s dV_{\xi} \frac{B(\underline{x}, \underline{\xi})}{4\pi r^2} Q_n(\underline{\xi}) \quad , \quad (1)$$

where $Q_n(\underline{\xi})$ is the neutron source strength and $B(\underline{x}, \underline{\xi})$ is the beam-attenuation kernel for the optical path connecting the points \underline{x} and $\underline{\xi}$. If the shield consists principally of water, this kernel is given by

$$B(\underline{x}, \underline{\xi}) = N(\rho) \exp \left[- \int_0^{\rho} dt \sigma_r(t) \right] \quad (2)$$

where

$N(\cdot)$ is the measured beam-attenuation kernel for water,

ρ is the effective thickness of water, at unit density, between the points \underline{x} and $\underline{\xi}$,

and

$\sigma_r(\cdot)$ is the removal cross section of the other materials traversed by the ray.

A similar expression,

$$\underline{J}_f(\underline{x}) = \int_s dV_{\xi} \frac{(\underline{x} - \underline{\xi})}{r} \frac{B(\underline{x}, \underline{\xi})}{4\pi r^2} Q_n(\underline{\xi}) \quad , \quad (3)$$

may be written for the current of fast neutrons. Since, in any case, the fast flux must be calculated in order to evaluate the effects of fast neutrons penetrating the shield, it is usually sufficiently accurate to utilize only Eq. (1) and to assume that the fast current is equal in magnitude to the fast flux and has the direction of its gradient. This procedure tends to overestimate the fast neutron current; however, it saves a considerable amount of numerical work. The fast current is needed in order to compute the thermal neutron flux distribution in the shield.

The computation of the thermal flux distribution is a relatively weak point in this scheme of shield design, and no generally accepted method exists for making such calculations. A reasonable procedure is to compute the negative of the divergence of the fast current and to take this to be the source term in a thermal neutron diffusion equation of the usual form, solvable by standard methods. If as is often the case, the fast neutron attenuation along a ray is nearly exponential, this practically amounts to taking the thermal neutron source to be the removal cross section times the fast

current. The thermal flux so obtained is used to calculate gamma-ray source densities in the capturing materials. Implicit in such a treatment of the slowing down process is the assumption that the lower energy components of the fast neutron flux are attenuated more strongly than the higher energy components.

The assumption of straight-ray propagation is again introduced for the gamma radiation; the dose outside of the shield is determined by an integral expression which is identical in form to Eq. (1). The gamma-ray attenuation along the ray is here taken to be exponential with linear build-up, which means that the kernel B in Eq. (1) is, for this case, given by

$$B(\underline{x}, \underline{\xi}) = \left[1 + \int_0^R dt \sigma(t) \right] \exp \left[- \int_0^R dt \sigma(t) \right], \quad (4)$$

where $\sigma(\cdot)$ is now the total photon collision cross section for the material traversed by the ray (Fig. 2). The dose contribution is calculated for each energy in the gamma-ray source spectrum and the results added.

III. DESIGN PROCEDURE AND SPECIAL PROBLEMS

The procedure followed in order to arrive at a fixed shield design was to compute, in the following sequence, the fast neutron flux, thermal neutron flux, and gamma-ray flux. This was first done for a preliminary arrangement of moderator and reactor vessel in order to estimate the magnitude of the nuclear heating in the vessel wall and to determine the amount of thermal shielding necessary.

When the reactor vessel and thermal shield arrangement were determined, the fluxes were extended and the heating in the concrete was established. The concrete heating was adjusted by adding lead until it was at a satisfactory level. As increasing the thickness of the lead also decreases the total concrete thickness to some extent, the total amount of lead chosen was the result of a combination of these two factors.

Final selection of the concrete thickness was made after the composition of the inner regions had been specified. This choice naturally included some factor of safety. Pessimism injected into the calculations served this purpose, as well as rounding off the concrete thickness to an even number of feet.

A similar procedure was followed to determine the shield thickness above and below the reactor core; however, there was not unlimited space in these directions. Shield design was thus somewhat limited to what material could best be placed in the available space.

Above the core there were 12 inches of space available for material which was to be selected solely on the basis of its shielding value. The remainder of the shield material in this region was selected primarily for purposes other than shielding. The result was an inordinate amount of iron in the shield. While from a shielding standpoint this does not appear to be a very efficient selection of materials, it presents very little problem in the light water-moderated reactor, as the fluxes are not excessive. Doubts do arise because of the lack of moderating material. In such a shield the predominant effect on the fast neutrons is that of inelastic scattering. This reduces the neutron energy, but not to thermal levels, and therefore is not consistent with the theory of attenuation involved; thus, the results cannot be considered completely accurate. To partially make up for this lack of moderator, ordinary concrete was selected as the most convenient material.

Operation as a heavy water-moderated reactor results in an increase in neutron fluxes, and the lack of moderation in the shield above the reactor core becomes more critical. Accordingly, it was then decided to use water as the moderating material. While heavy concrete is, in general, a more effective shield, and, by this type of calculation looks more efficient than water, it must be remembered that inconsistencies with the theory serve to make the calculation subject to greater suspicion. It is doubtful whether any calculations can accurately evaluate the situation; however, measurements during operation as a light water-moderated reactor may yield information that could shed some light on this problem. Due to the fact that other steel structure above the reactor shield reduced the radiation level from that which was calculated, and that streaming from voids and cracks increased the radiation level from that which was calculated, it may be difficult to decide even then what the best material for the shield should have been.

After some study of the vessel heating above the core and reflector region during heavy water-moderated operation, it was decided to include a borated steel plate above the core but just below the water level. This steel plate replaces the portion of the borated steel thermal shield that extends above the water level. It should aid in reducing capture gamma rays from the steel above the core as well as in protecting the vessel itself. In addition, the problem of cooling a thermal shield extending above the water level is avoided.

The shield design below the core was limited by the materials that could best be utilized in the four-foot space available. The reason for the four-foot thickness is that the control rods penetrate this region and it is advantageous to keep them as short as possible. Under the circumstances heavy concrete seemed the obvious choice and, accordingly, the design procedure was very much the same as for the radial shield.

Hope of attaining radiation levels that personnel might endure in the sub-pile room during operation is rather slim because of the numerous

penetrations. A primary consideration is that of equipment activation and, at least in the light water-moderated version, this does not appear to be a problem. The radiation level after shutdown is also of concern; this may be reduced to permissible levels by placing lead below the penetrations through which the forced circulation pipes pass. The maximum thickness of this lead is estimated to be eight inches, but it is recommended that this be determined empirically after operational experience has been accumulated.

Other shielding problems include those of compensating for voids caused by piping or structural considerations. The procedure used was to keep a constant shield density on a line of sight from core to shield exterior. While this has but little theoretical justification, it will suffice if care is taken that no unreasonable shield arrangements occur. For instance, reducing the shield to lead in any given direction would not be economical, nor would it be likely to produce an adequate shield.

IV. SHIELD DESIGN CALCULATIONS

A. Fast Neutron Flux

1. Light Water-Moderated EBWR

The fast neutron flux for the light water-moderated version of the EBWR was calculated on the basis of "removal theory," as described in Section II

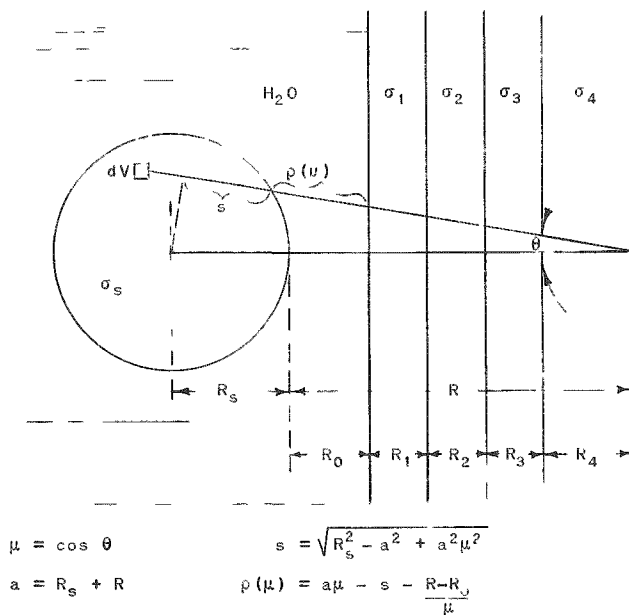


FIG. 3
SPHERICAL SOURCE WITH SLAB SHIELD

of this report. The geometrical configuration chosen to represent the problem was that of a spherical core surrounded by moderator and shielded with infinite slab shields (see Fig. 3). In addition, the core was assumed to be relatively opaque to fast neutrons. The expression for the fast neutron flux [Eq. (1)] thus becomes

$$\Phi_f(R) = \frac{Q_n K_n}{2\sigma_s} \int_{\mu_0}^1 d\mu N[\rho(\mu)] \exp\left[-\frac{1}{\mu} \sum_{i=1}^n \sigma_{ri} R_i\right] \text{ n/cm}^2 \text{ sec} \quad (5)$$

While the selection of an ordinary concrete shield is not consistent with the theory as represented, it is felt that ordinary concrete is enough of a moderator to be represented as such. Supporting this use is the fact that the measured relaxation length for fast neutrons in ordinary concrete⁽¹³⁾ approximates the reciprocal of the calculated removal cross section (0.091 cm^{-1}). In the axial direction, the heavy concrete in the bottom shield represents a greater deviation from fulfilling the requirements of the theory, but the method is applied with hope that, with the usual pessimism involved, it is not an underestimate. The cross section for the heavy concrete was derived from the measured relaxation length of fast neutrons in Brookhaven heavy concrete.⁽¹³⁾ In the axial direction above the reactor the great amount of iron also represents a deviation from the theory, but it is felt to be an adequate shield as discussed in Section III.

The shield configurations on the reactor core center lines in the three directions considered are given in Table I, along with the constants pertinent to the calculation. The source term at 20-mw operation power is

$$Q_n = \frac{20 \times 10^6 \text{ (watts)}}{\text{Volume (cm}^3\text{)}} = 14 \text{ watts/cm}^3$$

and is assumed to be a uniformly distributed isotropic source. The value of K_n is $69.4 \text{ (n/cm}^2 \text{ sec)}/(\text{mrep/hr})$. The function $N(\rho)$ has the dimensions $(\text{mrep/hr})/(\text{watt/cm}^2)$.^(8, 13) The fast neutron flux is, then, in units of $\text{n/cm}^2 \text{ sec}$. Figure 4 shows a section of the reactor vessel and shield. The fast neutron flux distributions in the three directions are given in Fig. 5. At the outer shield surface the fast neutron flux is 1×10^{-2} , 5×10^{-1} , and $1 \times 10^{-3} \text{ n/cm}^2 \text{ sec}$ in the directions radial, axial above the core, and axial below the core, respectively. The spectrum of neutrons involved is initially the fission spectrum, and, at the shield outer surface, the fission spectrum as degraded by the shield materials. Effectively, this is assumed to be represented by 2-Mev neutrons as far as human tolerance is concerned. This means that the permissible fast neutron flux is $40 \text{ n/cm}^2 \text{ sec}$.

2. Heavy Water-Moderated EBWR

The calculation of the fast neutron flux for the heavy water-moderated version of the EBWR represents a still greater deviation from the "removal theory" described. A possible justification for its use is that the reduction of the total cross section to removal cross section may be

Table I

CONSTANTS USED FOR THE CALCULATION OF THE FAST
NEUTRON FLUX IN LIGHT WATER-MODERATED
EBWR SHIELDING

Material	Density, gm/cc	Thickness, cm	Removal Cross Section, cm ⁻¹
<u>Radial Shield</u>			
Core	-	70	0.1642
Light Water	0.8	30.5	-
Steel	7.85	6.35	0.1635
Insulation	0.0	7.62	0.0
Helium	0.0	7.62	0.0
Lead	11.1	7.62	0.1122
Concrete (Ordinary)	2.4	244.	0.0901
<u>Axial Shield Above Core</u>			
Core	-	70	0.1642
Light Water	0.6	137.16	-
Steam	0.0	292.10	0.0
Steel	7.85	60.96	0.1635
Concrete (Ordinary)	2.4	30.5	0.0901
<u>Axial Shield Below Core</u>			
Core	-	70	0.1642
Light Water	0.8	104.14	-
Steel	7.85	6.35	0.1635
Insulation	0.0	7.62	0.0
Helium	0.0	13.97	0.0
Lead	11.1	7.62	0.1122
Concrete (Ordinary)	2.4	122.	0.0901
(Magnetite & Steel Punchings)	4.26	122.	0.1587

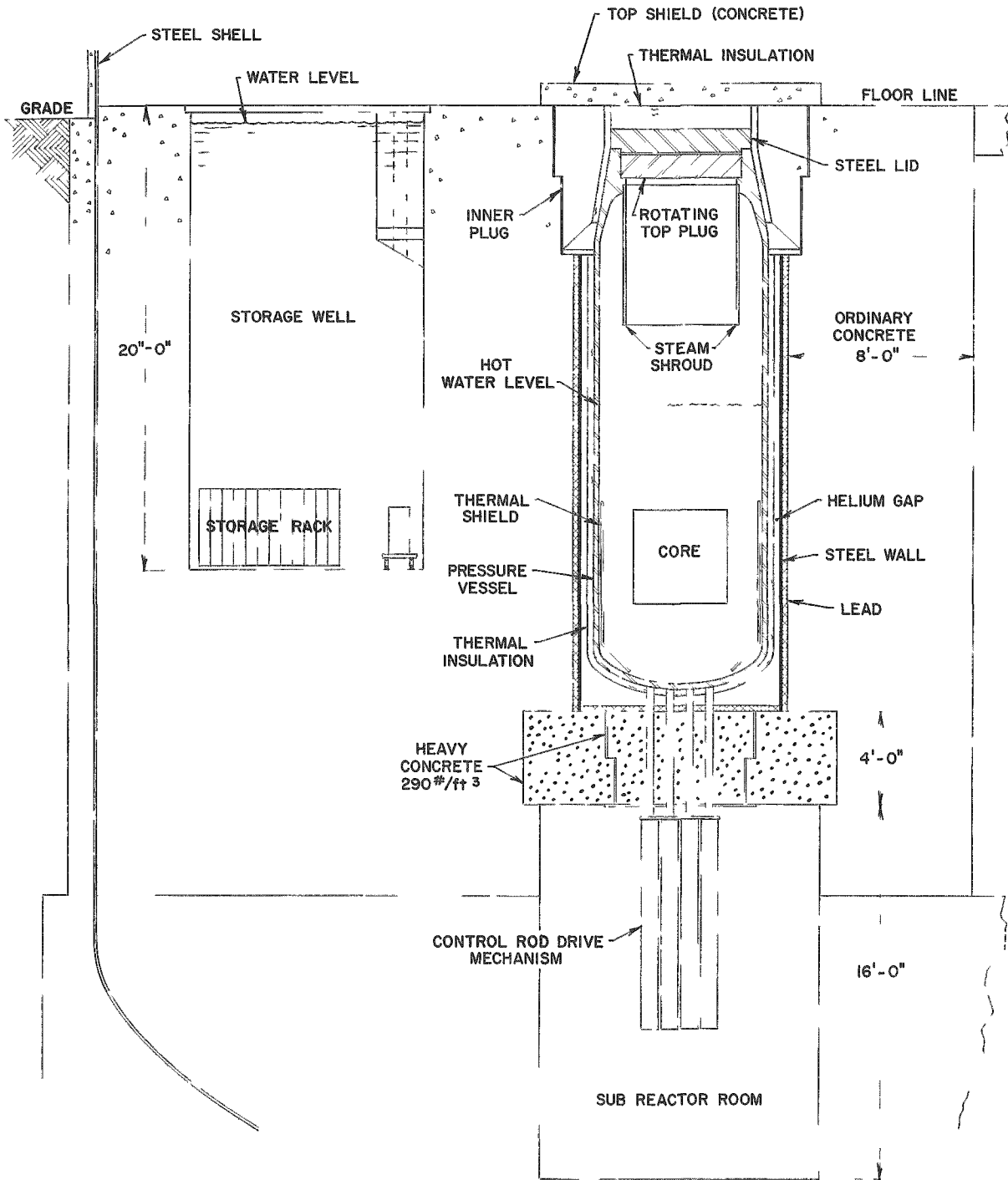


FIG. 4
VERTICAL SECTION OF THE LIGHT WATER MODERATED
EBWR VESSEL AND SHIELD

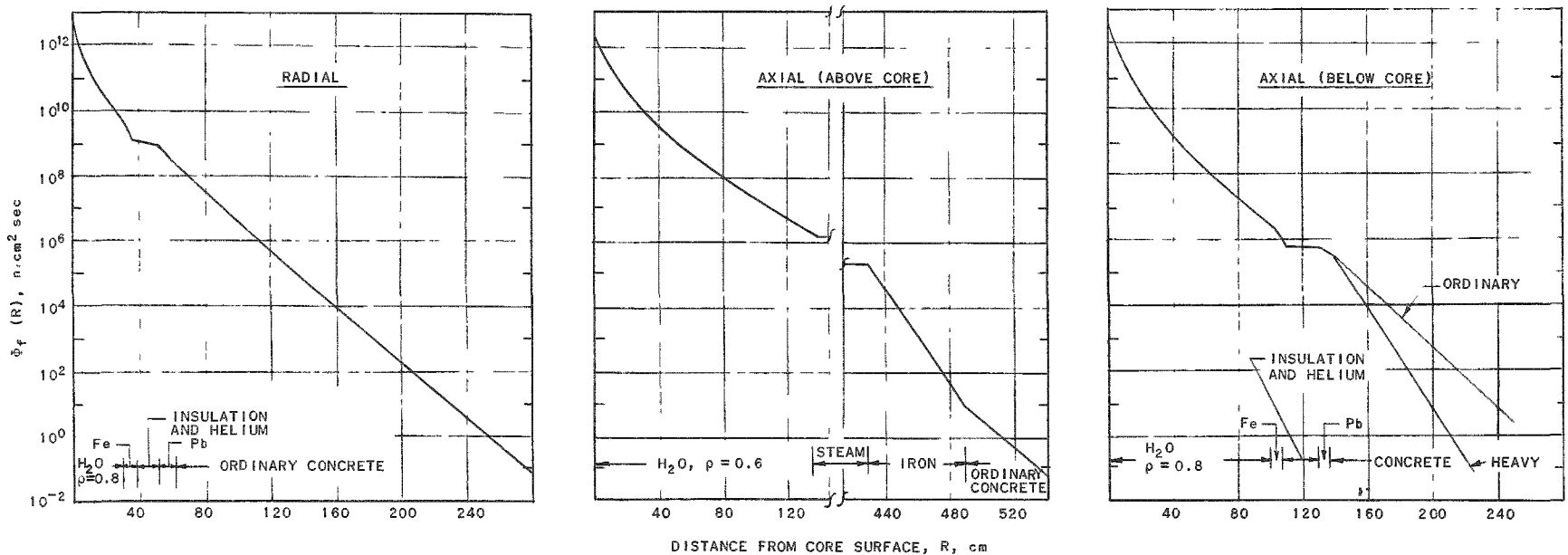


FIG. 5
CALCULATED FAST NEUTRON FLUX IN THE EBWR SHIELD (H_2O REFLECTOR)

looked upon to represent a method of estimating the buildup of fast neutrons as given by experimental methods. It is felt that this would give results representative of the fast neutron flux distribution, and this attitude is supported by the fact that there is no clearly correct way available to compute the fast neutron flux in such a situation. The function $N(\rho)$ in Eq. (5) is replaced by $e^{-\sigma_0 \rho}$, where σ_0 is the removal cross section for D_2O .

The shield configuration as modified for operation as a heavy water-reflected reactor is given in Fig. 6. The constants and the shield thickness are listed in Table II. The source strength, based on 40-megawatt operation, is

$$Q_n = \frac{40 \times 10^6 \times 3.1 \times 10^{10} \times 2.5}{\text{Volume}} = 2.2 \times 10^{12} \text{ n/cm}^3 \text{ sec} .$$

This is expressed in units different than the light-water source term because the kernel $N(\rho)$ is not used, and it did carry dimensions. The fast neutron flux distributions in the three directions are given in Fig. 7. The fluxes on the reactor core centerline at the outer shield surfaces are 1×10^{-1} , 10^1 to 10^2 , and 3×10^{-1} n/cm² sec in the directions radial, axial above the core, and axial below the core, respectively.

B. Thermal Neutron Flux

1. Light Water-Moderated EBWR

The thermal neutron flux distributions were computed by means of the one-group diffusion equation in slab geometry. The source term, as discussed in Section II, is the negative divergence of the fast neutron current. The simplifying assumption that the fast neutron flux is the same as the fast neutron current was included. The source term was represented by an exponential in all cases. The equation thus obtained for the thermal neutron flux is

$$\Phi_s(x) = A_i e^{+\kappa_i x} + B_i e^{-\kappa_i x} + C_i e^{-\sigma_i x} \text{ n/cm}^2 \text{ sec} \quad (6)$$

where

$$C_i = \frac{\sigma_i \Phi_{fi}(0)}{D_{si} (\kappa_i^2 - \sigma_i^2)} ,$$

and A_i and B_i are the arbitrary coefficients for the region i .

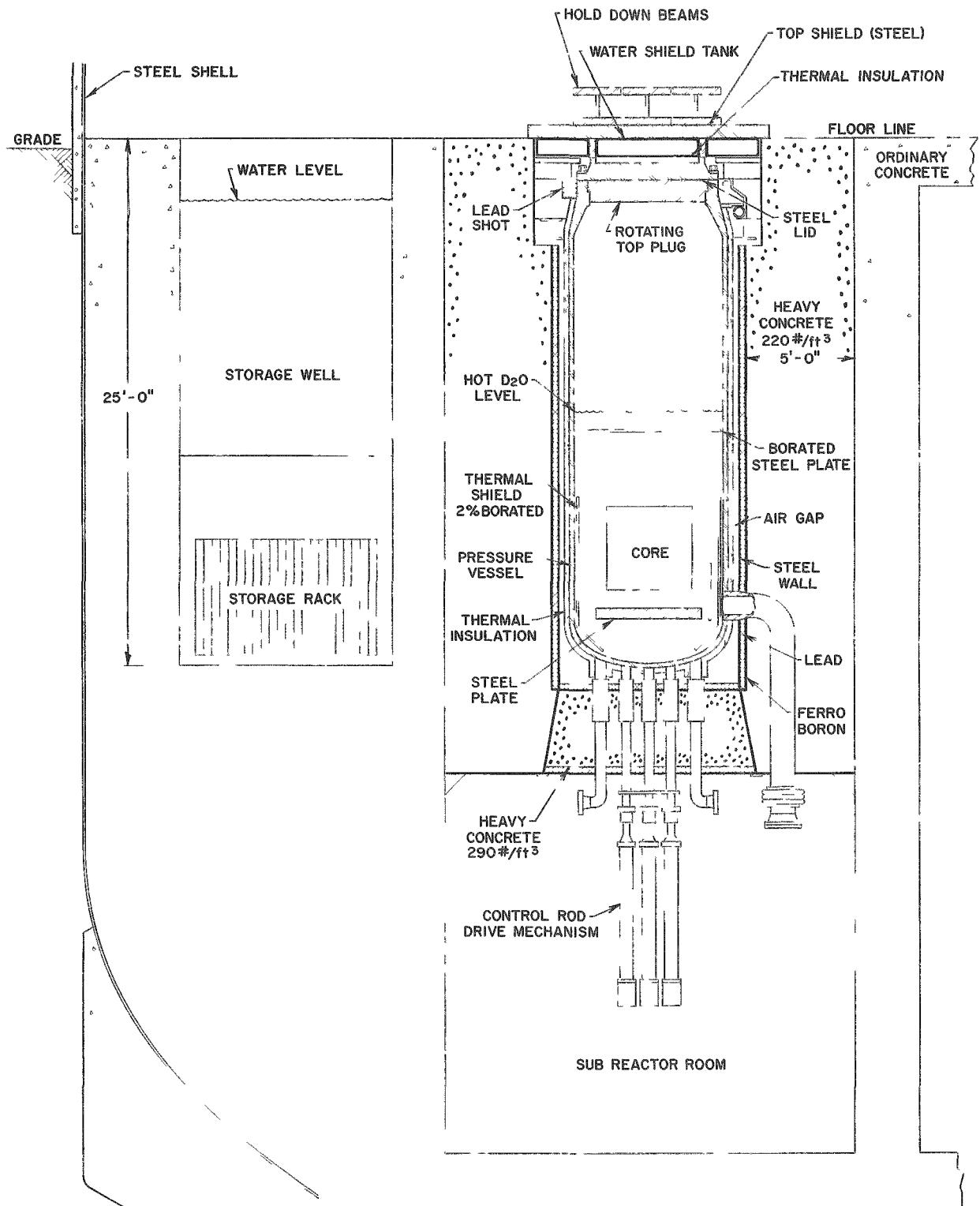


FIG. 6
 VERTICAL SECTION OF THE EBWR VESSEL AND SHIELD AS ALTERED
 TO INCLUDE OPERATION AS A HEAVY WATER MODERATED REACTOR

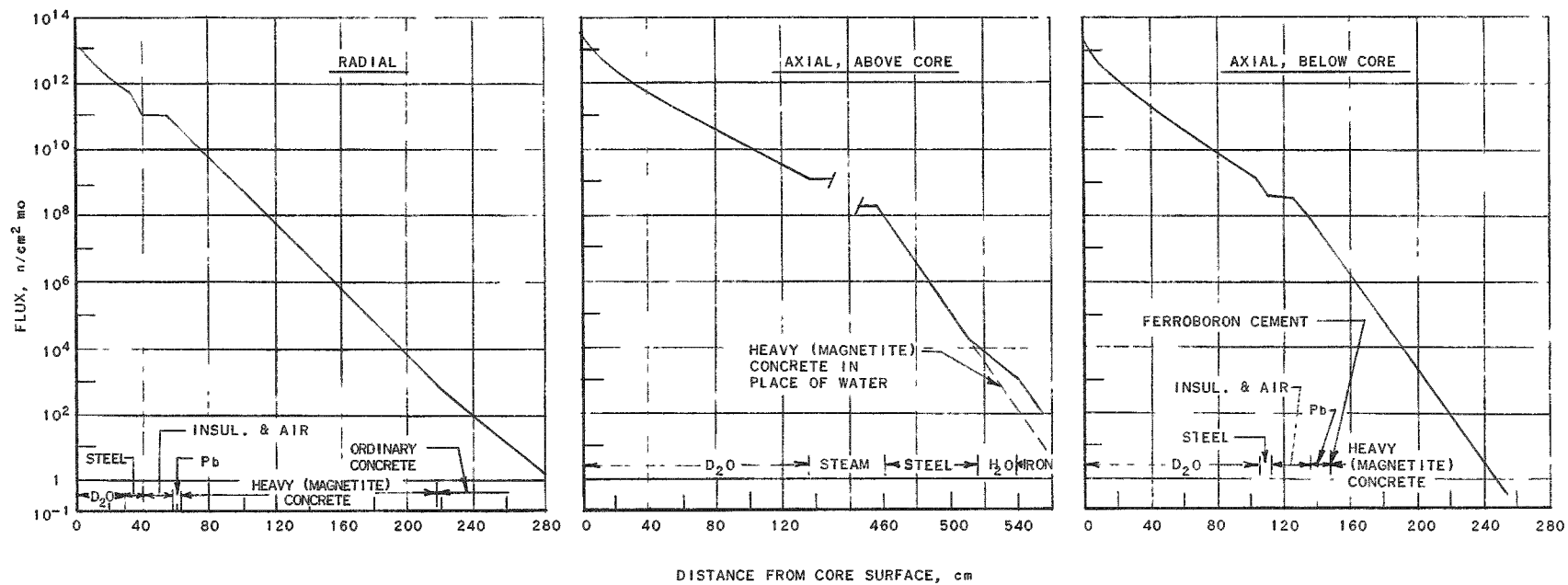


FIG. 7
CALCULATED FAST NEUTRON FLUX IN THE EBWR SHIELD (D₂O REFLECTOR)

RE-7-17025-B

Table II
 CONSTANTS USED FOR THE CALCULATION OF THE FAST
 NEUTRON FLUX IN HEAVY WATER-MODERATED
 EBWR SHIELDING

Material	Density, gm/cc	Thickness, cm	Removal Cross Section, cm ⁻¹
<u>Radial Shield</u>			
Core	-	70	0.0760
Heavy Water	0.8	30.5	0.0760
Steel (Borated)	7.85	2.54	0.1635
Steel	7.85	6.35	0.1635
Insulation	0.0	7.62	0.0
Air	0.0	7.62	0.0
Lead	11.1	7.62	0.1122
Concrete (Magnetite)	3.2	152.5	0.102
Concrete (Ordinary)	2.4	91.5	0.0901
<u>Axial Shield Above Core</u>			
Core	-	70	0.0760
Heavy Water	0.66	137.16	0.0760
Steam	0.0	320.0	0.0
Steel	7.85	55.88	0.1635
Light Water or Concrete (Magnetite & Steel Punchings)	1.0 4.26	25.4 25.4	0.0773 0.1587
Steel	7.85	17.78	0.1635
<u>Axial Shield Below Core</u>			
Core	-	70	0.0760
Heavy Water	0.8	104.14	0.0760
Steel	7.85	6.35	0.1635
Insulation	0.0	7.62	0.0
Air	0.0	7.62	0.0
Lead	11.3	7.62	0.1122
Concrete (Magnetite & Steel Punchings)	4.26	122.	0.1587

The boundary conditions imposed are that the thermal neutron flux at the core surface be given, that the thermal neutron flux and thermal neutron current be continuous at each shield interface, and that the thermal neutron flux be zero after an infinite thickness of the final region.

The use of slab geometry simplifies the computation very much, particularly when the work is done by hand. Several preliminary calculations were made to check the accuracy involved in the simplification of the geometry to that of infinite slabs. The methods utilized included spherical geometry, both by hand and by IBM CPC, slab geometry as described, and slab geometry as applied in the two-group diffusion equations. The spread of the thermal neutron fluxes was within a factor of two for the various methods employed. This included thermal neutron flux distributions calculated throughout the reflector, pressure vessel, and concrete regions of the EBWR. This study made the slab approximation seem relatively accurate as far as shielding calculations are concerned, and accordingly, the remainder of the computations were in the slab geometry.

The constants used to determine the thermal neutron flux distributions in the light water-moderated EBWR operated at 20 megawatts are listed in Table III. The resulting thermal neutron flux distributions are given in Figs. 8, 9, and 10.

Table III
CONSTANTS USED FOR THE CALCULATION OF THE THERMAL NEUTRON
FLUX IN THE LIGHT WATER-MODERATED EBWR SHIELDING

Material	Density, gm/cc	D_0 , cm	k_{eff} , cm ⁻¹	σ_a , cm ⁻¹	$\phi_f(0)$, r/cm ² sec
<u>Radial Shield</u>					
Light Water	0.8	0.2291	0.2256	0.1854	3.3×10^{12}
Steel	7.85	0.3604	0.6210	0.2012	4.3×10^9
Insulation & He	0.00293	7×10^2	3.3×10^{-4}	0.02112	1.2×10^9
Lead	11.1	0.9213	0.08346	0.1363	8.7×10^8
Concrete (Ordinary)	2.4	0.8452	0.08148	0.1045	3.1×10^8
<u>Axial Shield Above the Core</u>					
Light Water	0.6	0.3055	0.1693	0.1062	3.3×10^{12}
Steam	0.00293	7×10^2	3.3×10^{-4}	6.7×10^{-3}	1.6×10^6
Steel	7.85	0.3604	0.6210	0.1500	2.2×10^5
Concrete (Ordinary)	2.4	0.8452	0.08148	0.09295	8.0×10^0
<u>Axial Shield Below the Core</u>					
Light Water	0.8	0.2291	0.2256	0.1386	3.3×10^{12}
Steel	7.85	0.3604	0.6210	0.1319	1.8×10^6
Insulation & He	0.00293	7×10^2	3.3×10^{-4}	0.01143	5.8×10^5
Lead	11.3	0.9213	0.08346	0.07419	4.9×10^5
Concrete (Ordinary)	2.4	0.8452	0.08148	0.1008	2.8×10^5
Concrete (Magnetite & Steel Punchings)	4.26	0.4947	0.4402	0.1755	2.8×10^5

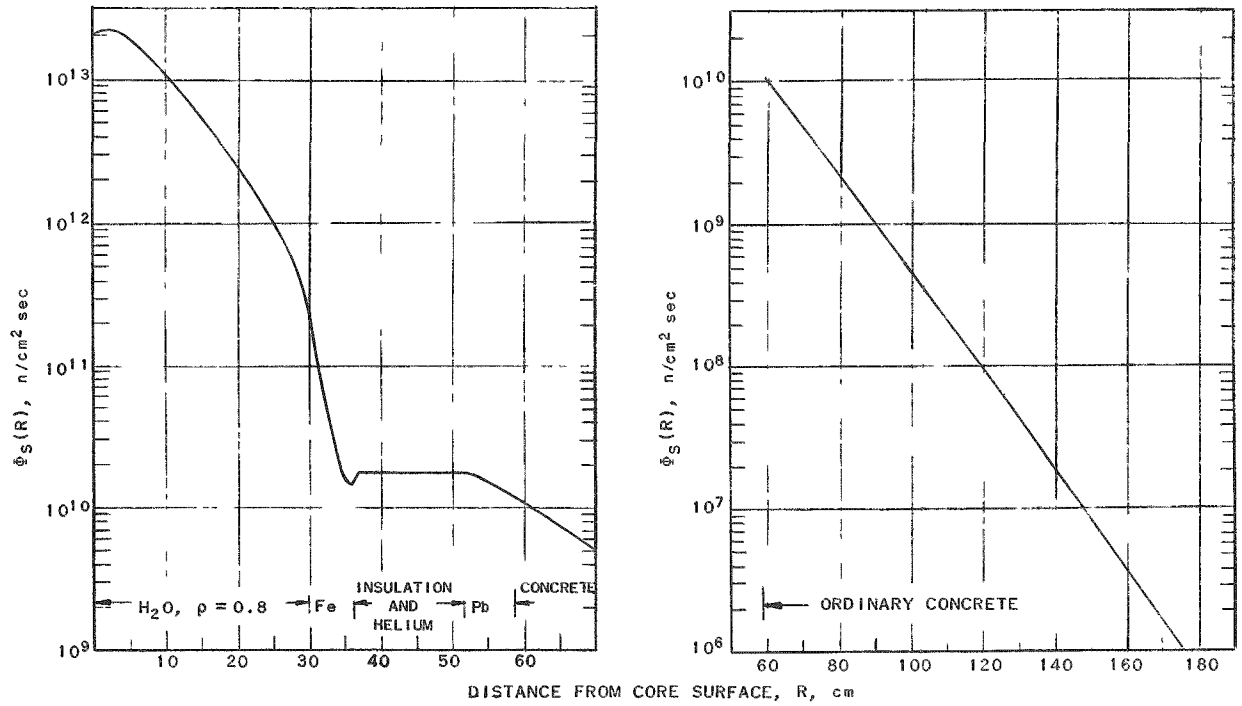


FIG. 8
CALCULATED THERMAL NEUTRON FLUX IN THE EBWR RADIAL SHIELD (H_2O REFLECTOR)

ANL-FWT-15847-A

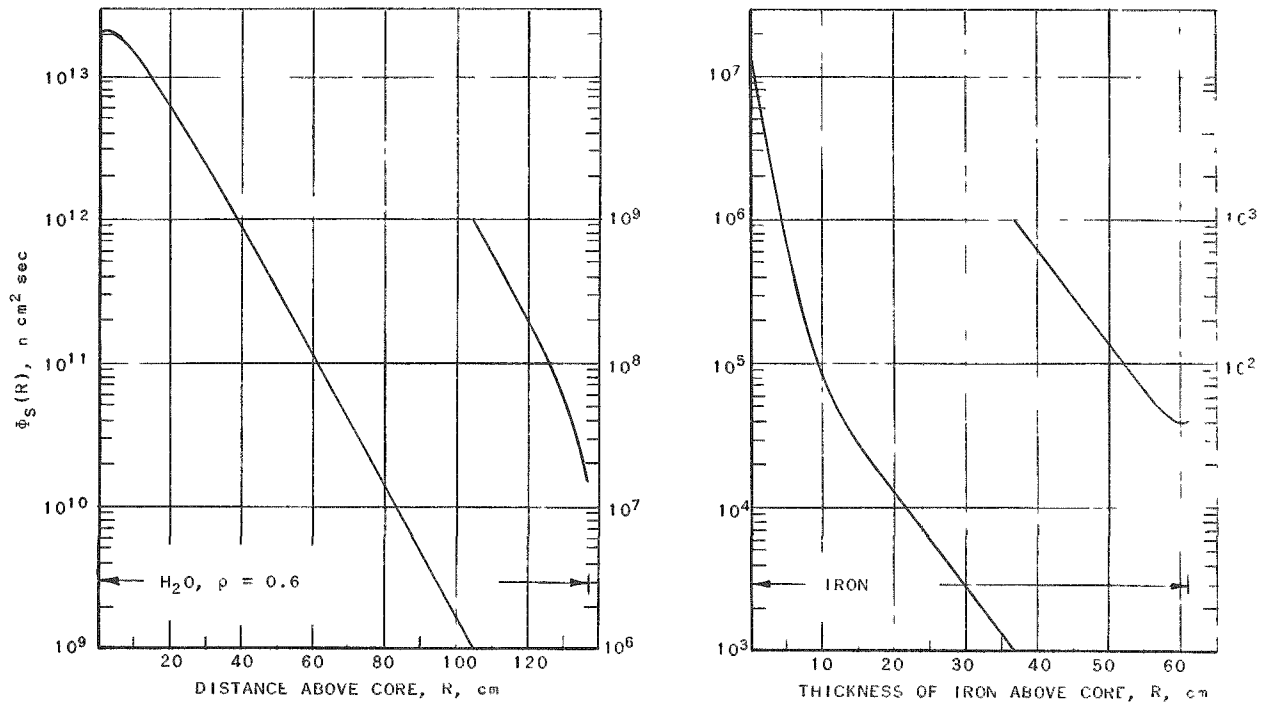


FIG. 9
CALCULATED THERMAL NEUTRON FLUX ABOVE THE EBWR CORE (F_2C REFLECTOR)

ANL-FWT-15845-A

RE-7-16212-J

24

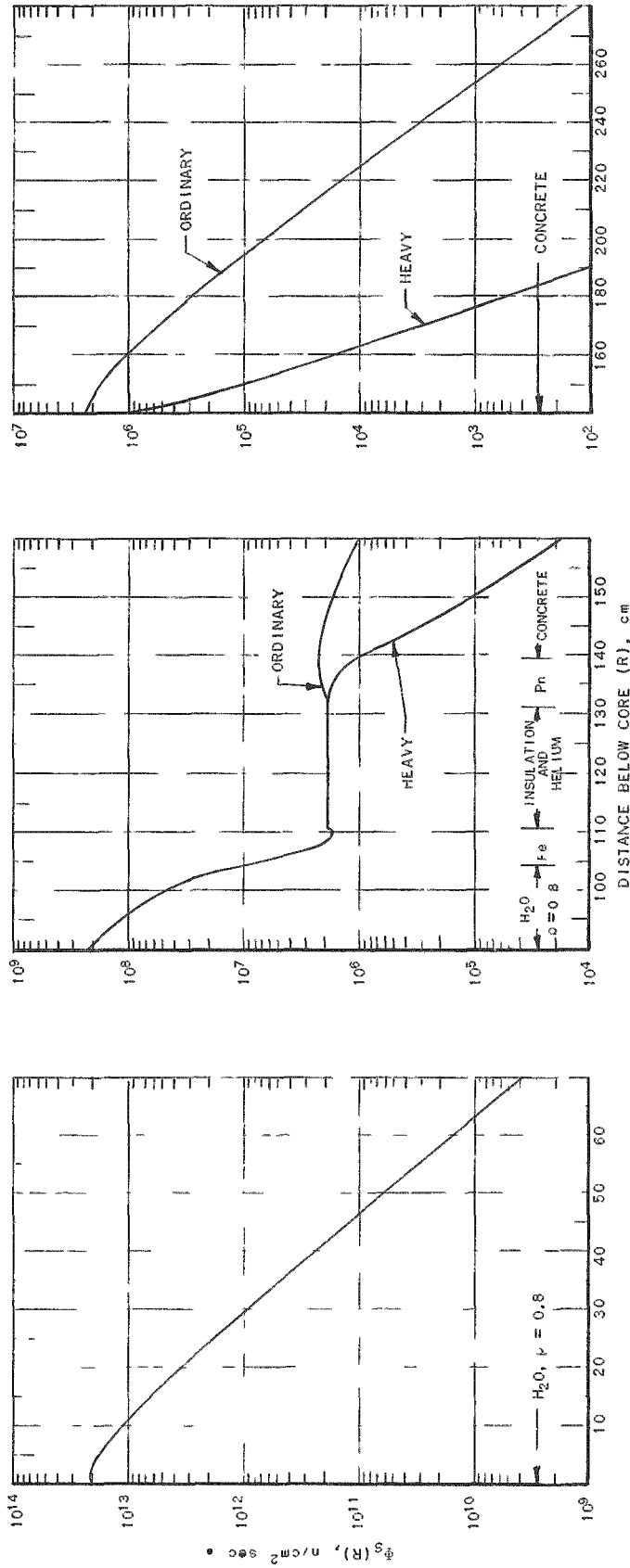


FIG. 10
CALCULATED AXIAL THERMAL NEUTRON FLUX BELOW THE EBWR CORE (H_2O REFLECTOR)

2. Heavy Water-Moderated EBWR

The method of calculating the thermal neutron flux distributions in the heavy water-moderated EBWR is the same as for the light water-moderated reactor. While the shield design for the heavy water-moderated EBWR was in progress, it soon became obvious that a judicious placement of boron would be quite beneficial. The boron-steel thermal shield and the boron-steel plate above the reactor are two such places already mentioned. In addition, a one-inch thick plaster made of ferroboron and Portland cement was placed between the lead and concrete in the radial shield and also in the shield below the core. All of these layers were treated as black boundaries, in so far as the thermal neutron flux was concerned, except for the 2% borated steel thermal shield. This region was assigned constants and a flux distribution calculated in order to estimate the capture gamma rays from iron absorptions occurring in the thermal shield. For comparison purposes, the thermal neutron flux is plotted both with and without these boron regions. A steel plate below the reactor core, which was neglected for the sake of pessimism in the fast neutron flux calculations, has been included in the thermal neutron flux calculation.

The constants used in the determination of the thermal neutron flux for the heavy water-moderated EBWR are listed in Table IV. The thermal neutron flux distributions are plotted in Figs. 11, 12, and 13. Note that, as for the fast neutron flux calculations, the power level assumed for the heavy water-moderated reactor is twice that for the light water-moderated reactor, or 40 megawatts.

C. Gamma-Ray Flux

The gamma-ray flux distributions throughout the shield were computed by means of formulas derived from the basic considerations in Section II. This included exponential attenuation with linear buildup.

The gamma-ray flux from sources located in the reactor core was deduced on the basis of the geometry represented in Fig. 3. Additional assumptions were that the source be constant throughout the core and that contributions from the far side of the core were negligible. On these bases the gamma-ray flux is

$$\Phi_{\gamma}(r) = \frac{Q_{\gamma}}{2\sigma_s} \int_{\mu}^1 d\mu \left[\left(1 + \sigma_0 \rho + \frac{1}{\mu} \sum_{i=1}^n \sigma_i R_i \right) \times \right. \\ \left. \exp \left(-\sigma_0 \rho - \frac{1}{\mu} \sum_{i=1}^n \sigma_i R_i \right) \right] \gamma / \text{cm}^2 \text{ sec} \quad (7)$$

Table IV

CONSTANTS USED FOR THE CALCULATION OF THE
THERMAL NEUTRON FLUX IN THE HEAVY
WATER-MODERATED EBWR SHIELDING

Material	Density gm/cc	D_s , cm	κ , cm^{-1}	σ , cm^{-1}	$\phi_f(0)$, $\text{n/cm}^2 \text{ sec}$
<u>Radial Shield</u>					
Heavy Water	0.8	1.104	0.0069	0.1198	2.0×10^{13}
Steel (2% B)	7.85	0.3015	4.7393	0.205	5.3×10^{11}
Steel	7.85	0.3604	0.621	0.205	3.1×10^{11}
Lead	11.3	0.9213	0.08346	0.136	8.5×10^{10}
Concrete (Ordinary)	2.4	0.8452	0.08198	0.106	3.0×10^{10}
or Concrete (Magnetite)	3.2	0.6051	0.293	0.1155	3.0×10^{10}
(Ordinary)	2.4	0.8452	0.08198	0.0958	6.8×10^2
<u>Axial Shield Above the Core</u>					
Heavy Water	0.6	1.47	0.00518	0.0710	2.0×10^{13}
Steel	7.85	0.3604	0.621	0.1677	1.7×10^8
Light Water	0.96	0.1913	0.2702	0.08130	1.4×10^4
Steel	7.85	0.3604	0.6210	0.1670	1.8×10^3
Steel	7.85	0.3604	0.6210	0.1677	1.7×10^8
Concrete (Magnetite & steel punchings)	4.26	0.4947	0.4143	0.1587	1.4×10^4
Steel	7.85	0.3654	0.6210	0.1670	2.6×10^2
<u>Axial Shield Below the Core</u>					
Heavy Water	0.8	1.104	0.0069	0.0920	2.0×10^{13}
Steel	7.85	0.3604	0.6210	0.0894	5.5×10^{11}
Heavy Water	0.8	1.104	0.0069	0.0783	2.25×10^{11}
Steel	7.85	0.3604	0.6210	0.1782	1.4×10^9
Lead	11.3	0.9213	0.08346	0.1462	3.8×10^8
Concrete (Magnetite & steel punchings)	4.26	0.4947	0.4143	0.1645	1.5×10^8

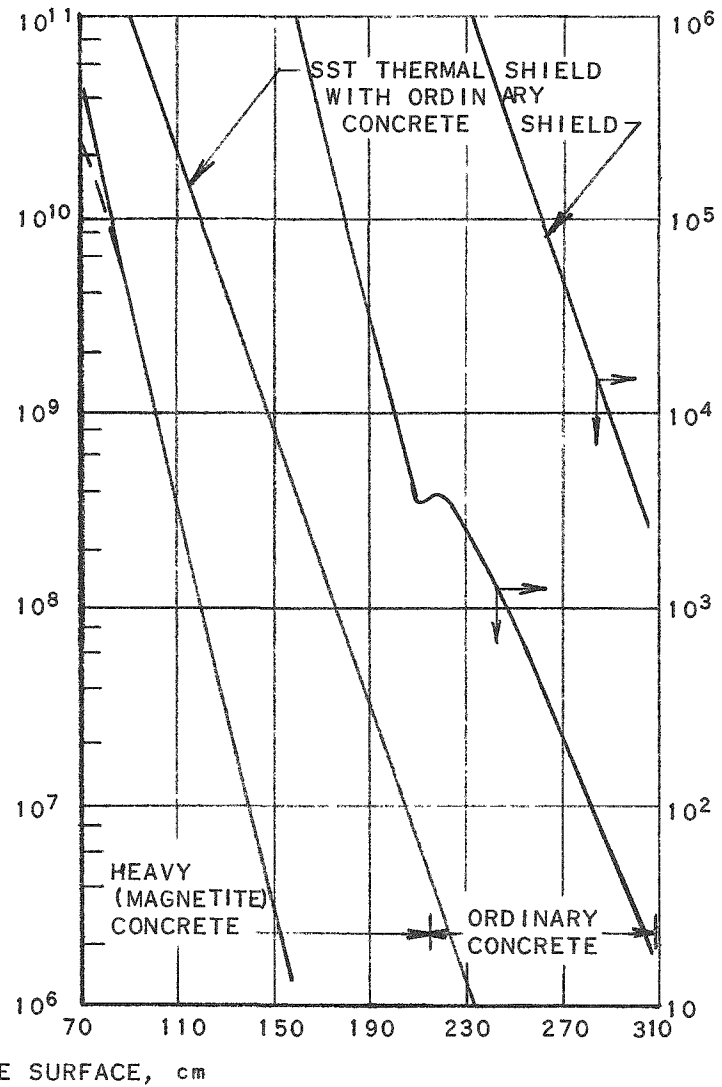
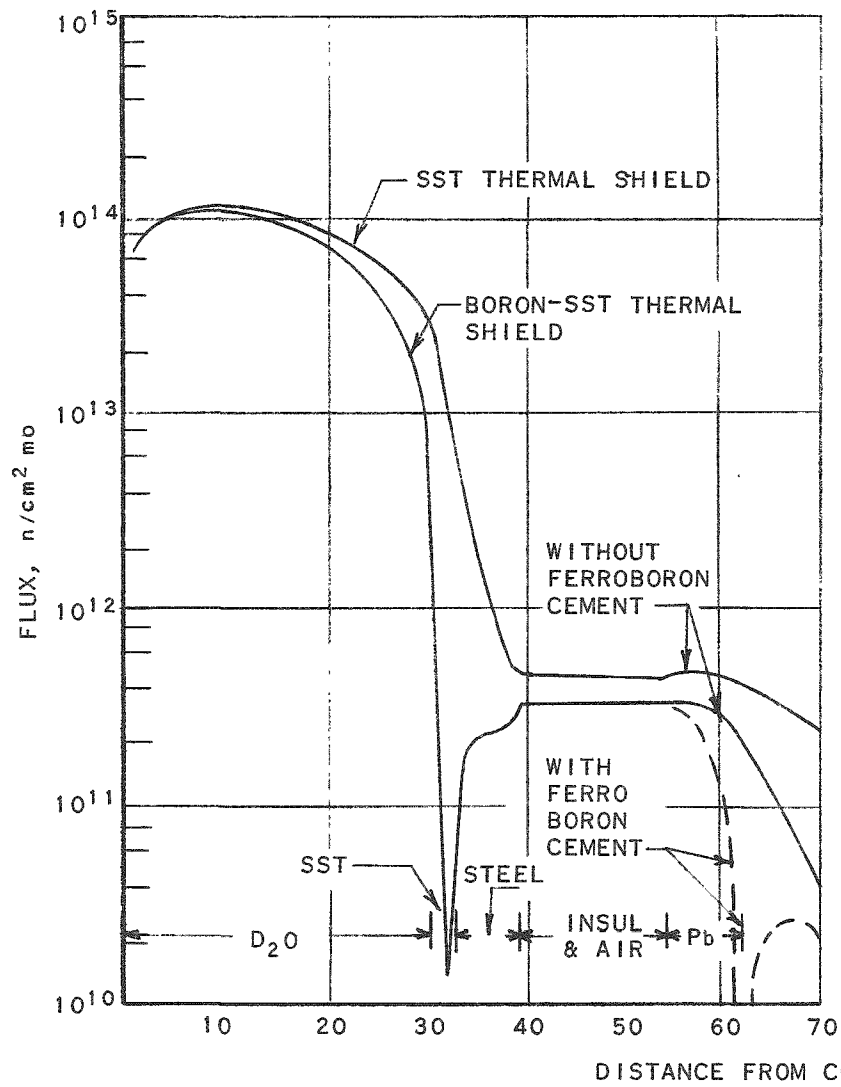


FIG. II
CALCULATED THERMAL NEUTRON FLUX IN THE EBWR RADIAL SHIELD (D_2O REFLECTOR)

RE-7-17015-A

28

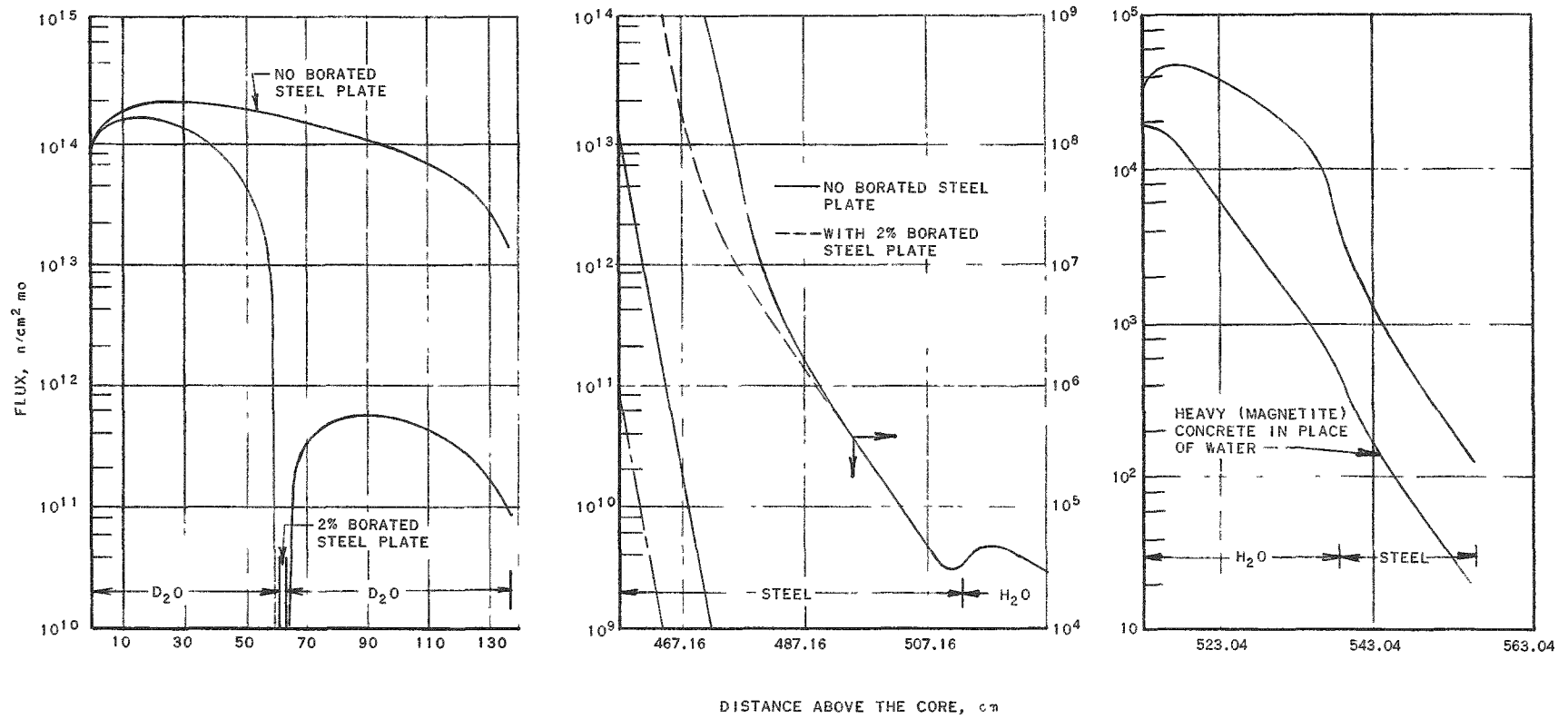


FIG. 12
CALCULATED THERMAL NEUTRON FLUX ABOVE THE EBWR CORE (D₂O REFLECTOR)

RE-7-17016-B

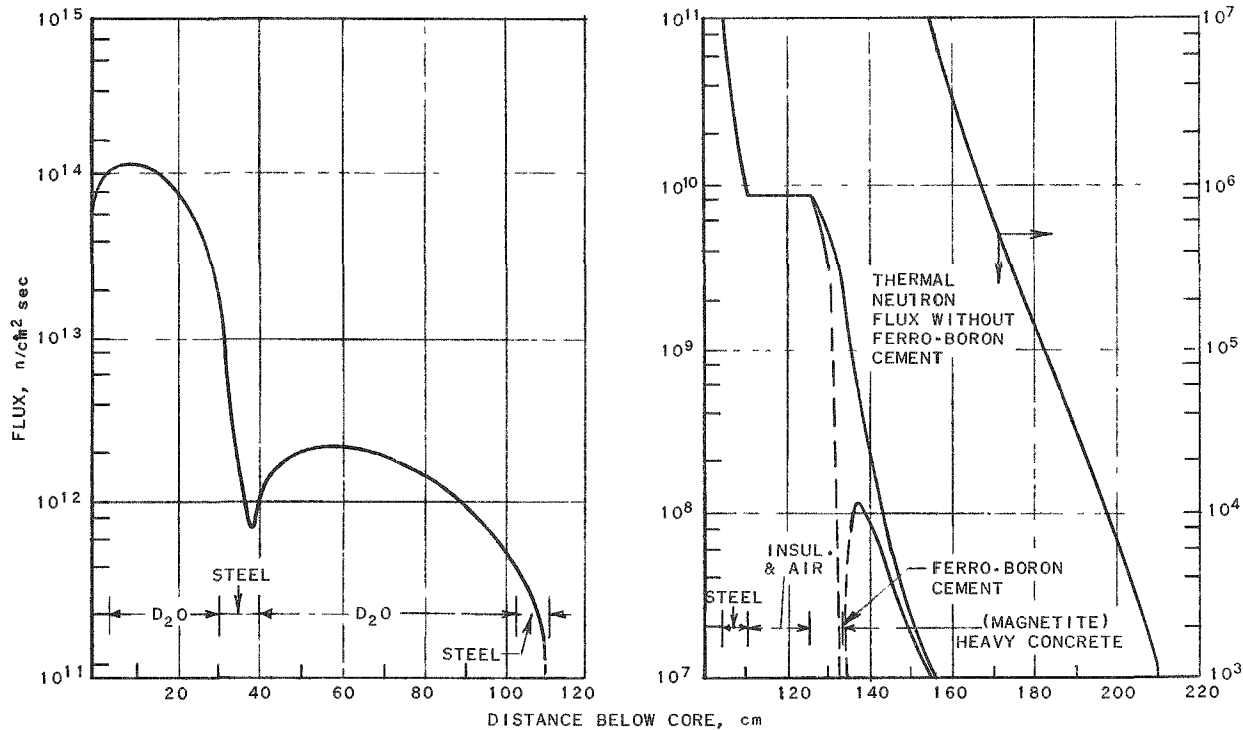


FIG. 13
CALCULATED THERMAL NEUTRON FLUX BELOW THE EBWR CORE (D₂O REFLECTOR)

RE-7-17023-A

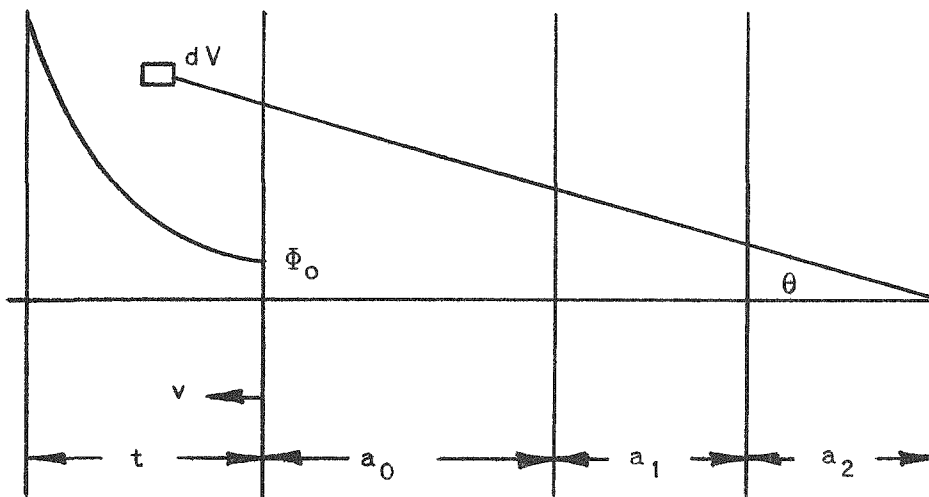


FIG. 14
GEOMETRY FOR PLANE VOLUME SOURCE WITH SLAB SHIELDS

The gamma-ray flux from sources outside the core, that is, neutron capture in shield materials, was computed on the basis of slab geometry as illustrated in Fig. 14.

For a source which is constant the expression for the gamma-ray flux is

$$\Phi(a) = \frac{Q_\gamma}{2\sigma_s} [2 E_2(\sigma a) - 2 E_2(\sigma_s t + \sigma a) + \sigma a E_1(\sigma a) - (\sigma_s t + \sigma a) E_1(\sigma_s t + \sigma a)] \gamma/\text{cm}^2 \text{ sec} \quad (8)$$

The source term " Q_γ " is the number of gamma rays born per cubic centimeter each second and is related to the thermal neutron flux

$$Q_\gamma = \sigma_a \Phi_s N_\gamma \quad .$$

The functions $E_n(x)$ are defined as

$$E_n(x) = \int_1^\infty du \frac{e^{-xu}}{u^n} \quad . \quad (9)$$

A complete discussion, tables of values, and integrals of the functions are contained in reports by Placzek⁽¹⁵⁾ and LeCaine.⁽¹⁶⁾ More complete tables of the first order E function, $E_1(x)$, are included in the WPA Tables⁽¹⁷⁾ under the nomenclature of Jahnke-Emde:

$$E_1(x) = -E_i(-x) \quad .$$

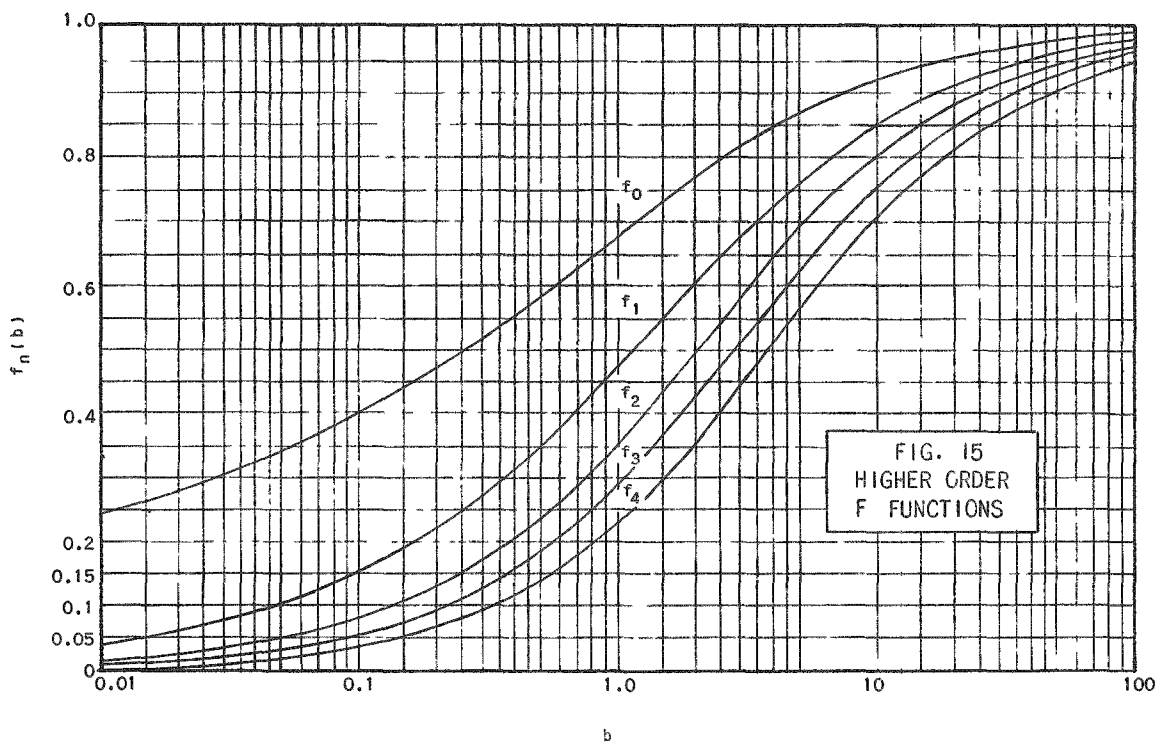
Convenient graphs are located in the Shielding Design Manual.⁽⁹⁾ The higher order E functions may be computed by means of the recursion formula:

$$E_n(x) = \frac{1}{n-1} [e^{-x} - x E_{n-1}(x)], \quad n > 1, \quad (10)$$

or by means of the formula

$$E_n(x) = \frac{e^{-x}}{x + n - 1 + f_{n-1}(x)}, \quad n \geq 1 \quad . \quad (11)$$

The graphs of $f_n(x)$ from the same report are reproduced here as Fig. 15.



The gamma-ray flux from a source which is exponentially distributed in the same slab geometry (Fig. 14) may be expressed:

where $\nu < 1$ as

$$\begin{aligned} \Phi(a) = & \frac{Q\gamma}{2k} \left[e^{kt} E_1(\sigma_{st} + \sigma a) - E_1(\sigma a) \right. \\ & + \frac{k}{(k - \sigma_s)} e^{-\sigma a} [e^{(k - \sigma_s)t} - 1] \\ & \left. + e^{-\nu \sigma a} \left\{ E_1[\sigma a(1 - \nu)] - E_1[(\sigma_{st} + \sigma a)(1 - \nu)] \right\} \right] \gamma/\text{cm}^2 \text{ sec}, \end{aligned} \quad (12)$$

or where $\nu > 1$ as

$$\begin{aligned} \Phi(a) = & \frac{Q\gamma}{2k} \left[e^{kt} E_1(\sigma_{st} + \sigma a) - E_1(\sigma a) \right. \\ & + \frac{k}{(k - \sigma_s)} e^{-\sigma a} [e^{(k - \sigma_s)t} - 1] \\ & \left. + e^{-\nu \sigma a} \left\{ E_i[(\sigma_{st} + \sigma a)(\nu - 1)] - E_i[\sigma a(\nu - 1)] \right\} \right] \gamma/\text{cm}^2 \text{ sec} . \end{aligned} \quad (13)$$

The source term is related to the thermal neutron flux as before:

$$Q_{\gamma}(v) = \sigma_a \Phi_s(v) N_{\gamma} \quad \gamma/\text{cm}^3 \text{ sec} \quad ,$$

but now the thermal flux is of the form

$$\Phi_s(v) = \Phi_0 e^{kv} \quad \text{n/cm}^2 \text{ sec} \quad .$$

Here " v " is a variable which is zero at the source shield interface and increases with distance into the source. While the thermal flux may not always be representable by a single exponential, it can always be represented by, at most, the sum of three exponentials, because the method of calculation has a maximum of three terms. The function $Ei(x)$ is tabulated in the WPA Tables⁽¹⁷⁾ and presented graphically in the Shielding Manual.⁽¹⁰⁾ It is defined as

$$Ei(x) = \int_{-\infty}^1 du \frac{e^{+xu}}{u} \quad . \quad (14)$$

The expression for the gamma-ray flux at the edge of a source which is exponentially distributed is also of use, and, because the formulas do not follow in a simple algebraic fashion by letting $a \rightarrow 0$ in Eqs. (12) and (13), they are reproduced.

For $\nu < 1$:

$$\begin{aligned} \Phi(t) = & \frac{Q_{\gamma}}{2k} \left\{ e^{kt} E_1(\sigma_s t) - \ln(1-\nu) - E_1[\sigma_s t(1-\nu)] \right. \\ & \left. + \frac{k}{(k-\sigma_s)} [e^{(k-\sigma_s)t} - 1] \right\} \quad \gamma/\text{cm}^2 \text{ sec} \quad . \end{aligned} \quad (15)$$

For $\nu > 1$:

$$\begin{aligned} \Phi(t) = & \frac{Q_{\gamma}}{2k} \left\{ e^{kt} E_1(\sigma_s t) - \ln(\nu-1) + Ei[\sigma_s t(\nu-1)] \right. \\ & \left. + \frac{k}{(k-\sigma_s)} [e^{(k-\sigma_s)t} - 1] \right\} \quad \gamma/\text{cm}^2 \text{ sec} \quad . \end{aligned} \quad (16)$$

The preceding formulas for the gamma-ray flux have been derived on the basis of monochromatic radiation. While this is rarely, if ever, a real situation, there are ways of approximating the spectrum to adapt it to these monochromatic formulas. A single effective energy may be chosen to represent the entire spectrum, or, still better, a series of effective energies or a line spectrum may be chosen. For this report the latter choice was made. Fission gamma rays were considered to be in either the 1-mev or the 2.5-mev energy range. The prompt fission gamma-ray energy was assigned to the 2.5-mev energy group and the fission product gamma-ray energy was assigned in the proportion 25% to the 1-mev

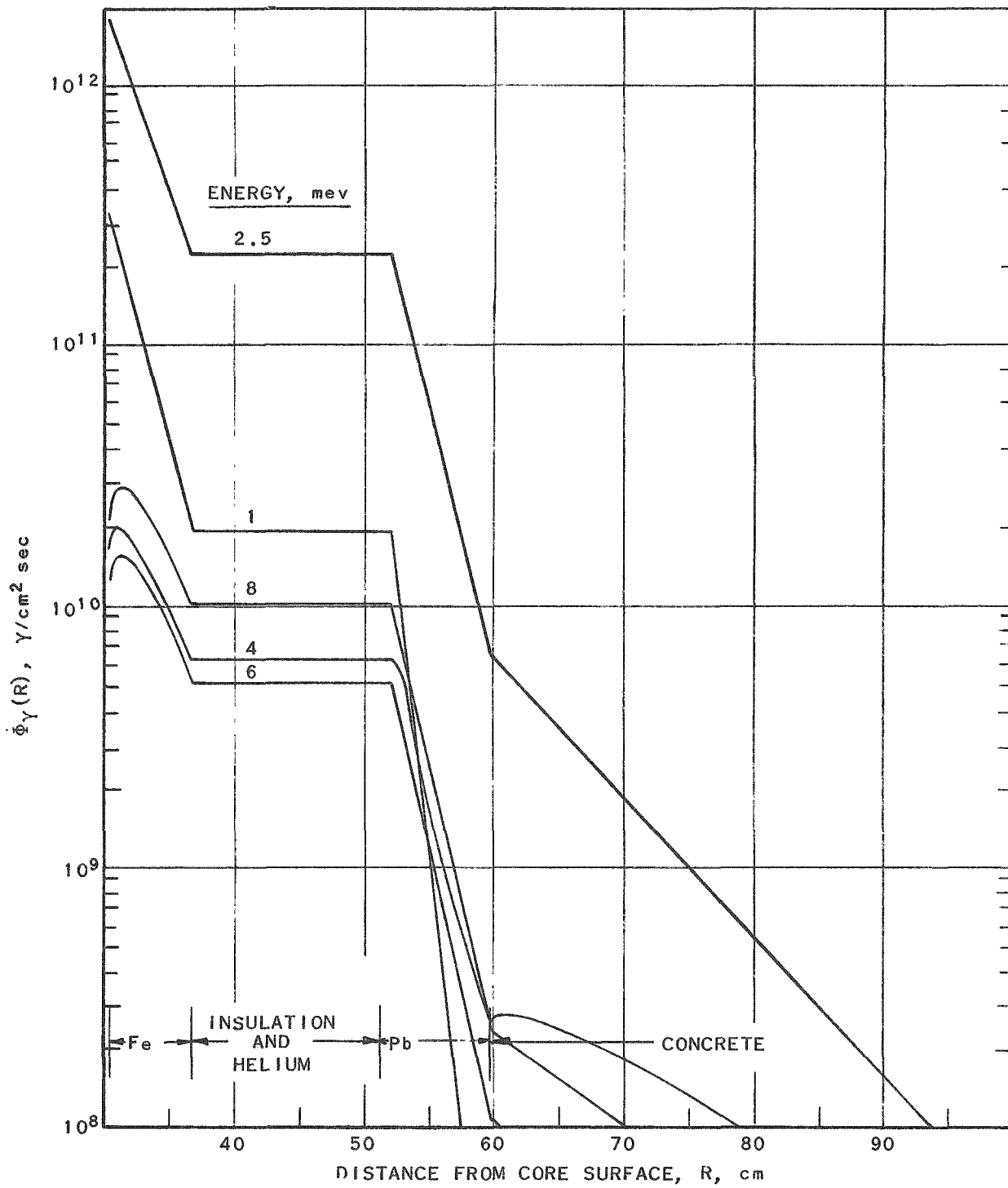
group and 75% to the 2.5-mev group. More detailed information concerning the spectra of these gamma rays may be found in the Shielding Manual.⁽¹¹⁾ Capture gamma-ray energy was assigned according to the NDA-NBS compilation.⁽¹⁹⁾ The net result is a line spectrum with lines at 1, 2.5, 4, 6, and 8 mev. The relative importance of each line depends upon the position in the shield; for example: the two lower energy lines were important in determining the heating in the vessel, and the two higher energy lines were important in determining total shield leakage.

The gamma-ray absorption coefficients⁽²⁰⁾ used in determining the shield design for the light water-moderated reactor are compiled in Table V. Gamma-ray fluxes are plotted in Figs. 16, 17, and 18.

Table V
GAMMA-RAY ABSORPTION COEFFICIENTS (H₂O REFLECTOR)
(in cm⁻¹)

Material	Density, gm/cc	Gamma-ray Energy, mev				
		1	2.5	4	6	8
Core	-	0.3429	0.2101	0.2086	0.1998	0.2081
Light Water	0.8	0.0565	0.0356	0.0271	0.0222	0.0194
Steel	7.85	0.4694	0.3069	0.2591	0.2394	0.2339
Lead	11.1	0.7803	0.4823	0.4618	0.4940	0.5228
Concrete (Ord.)	2.4	0.1524	0.09696	0.07608	0.06432	0.05832
(Magnetite & steel punchings)	4.26	0.2731	0.1737	0.1363	0.1152	0.1045

The gamma-ray fluxes in the heavy water-reflected reactor were computed in a similar manner. The gamma-ray absorption coefficients are listed in Table VI. The gamma-ray fluxes are plotted in Fig. 19.



ANL-FWT-15844-A

FIG. 16
CALCULATED GAMMA-RAY FLUX IN THE EBWR RADIAL SHIELD
(H₂O REFLECTOR)

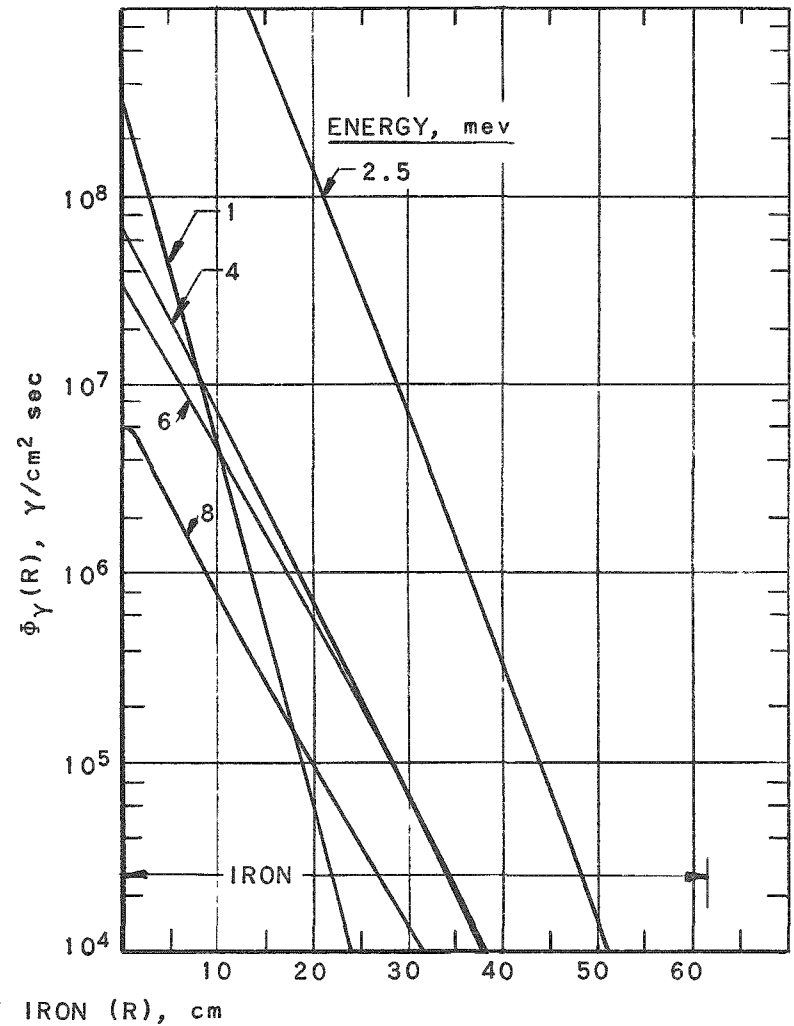
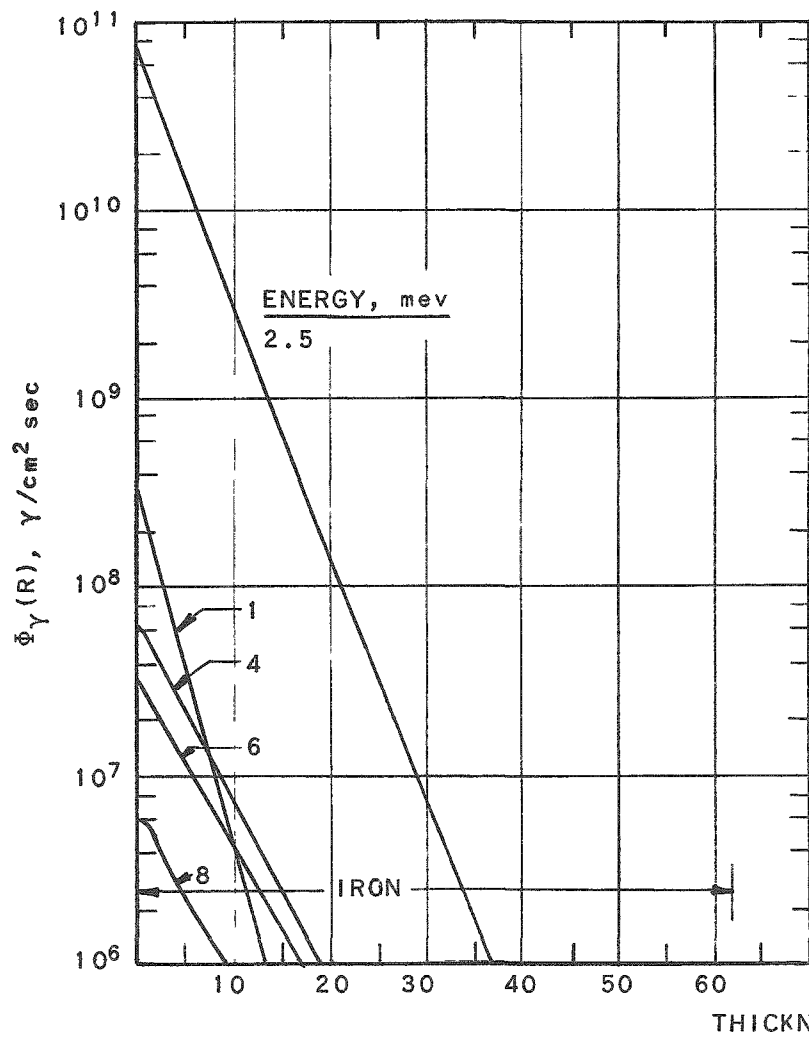


FIG. 17
CALCULATED GAMMA-RAY FLUX ABOVE THE EBWR CORE (H₂O REFLECTOR)

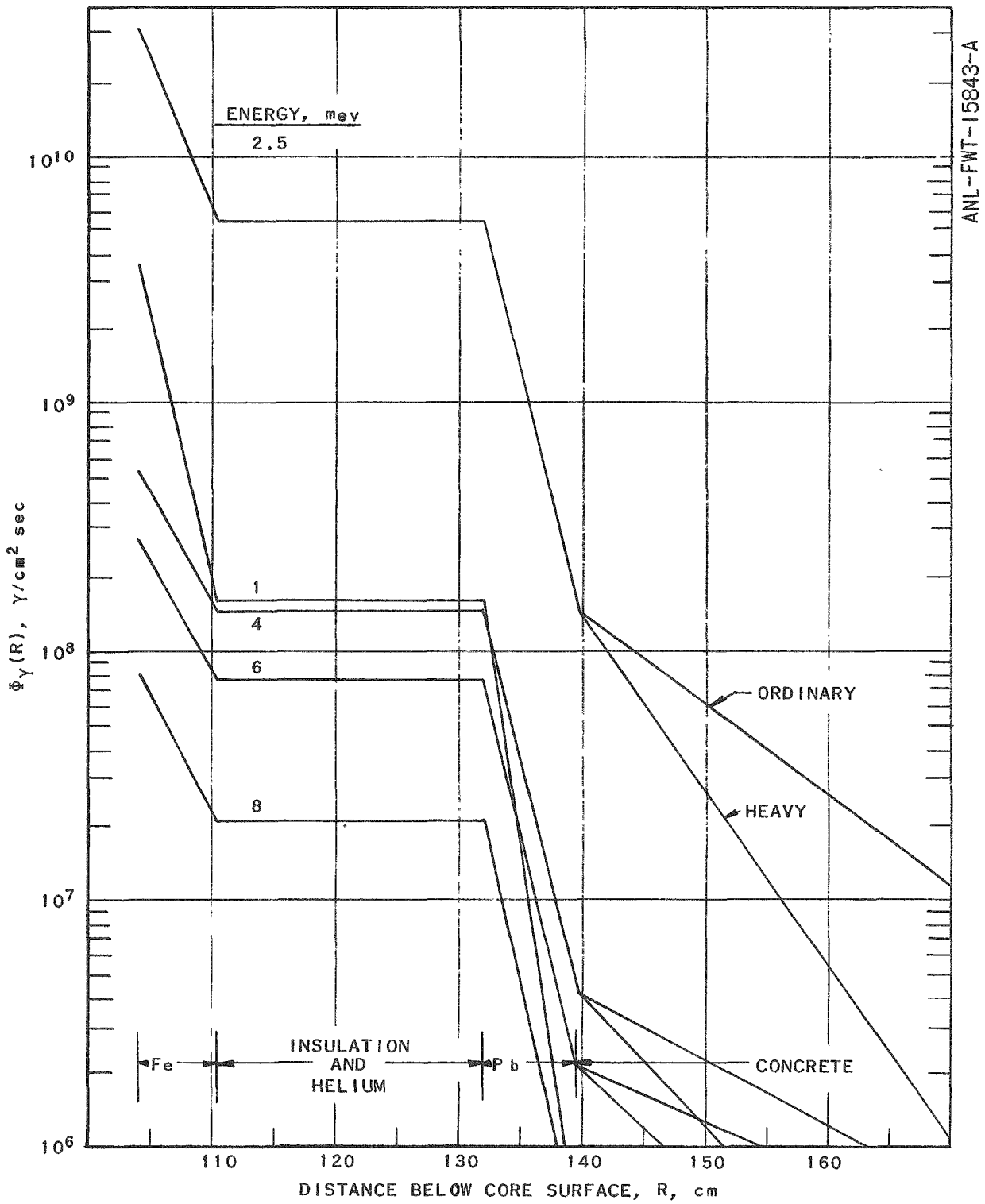


FIG. 18
CALCULATED GAMMA-RAY FLUX BELOW THE EBWR CORE
(H₂O REFLECTOR)

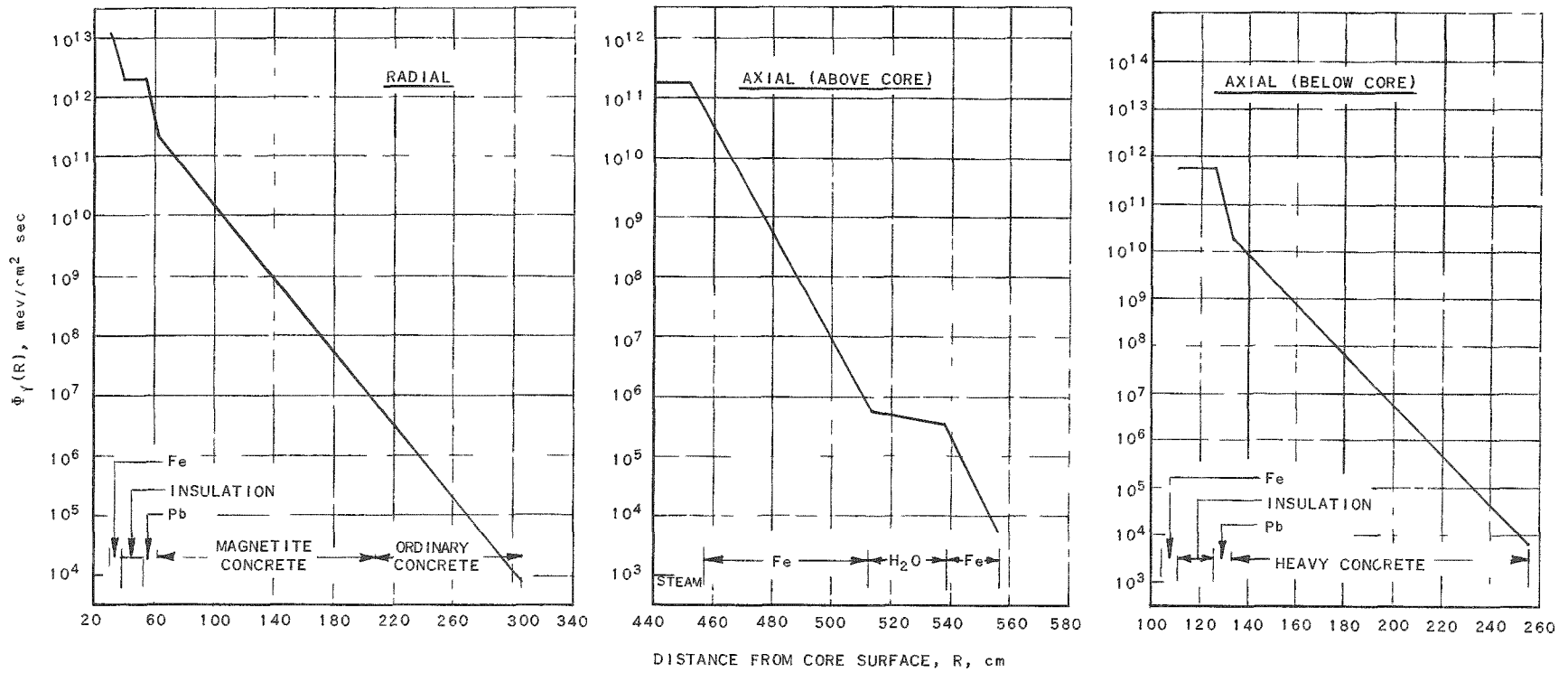


FIG. 19
CALCULATED GAMMA-RAY FLUXES IN THE EBWR (D_2O REFLECTOR)

RE-7-18654-B

Table VI
 GAMMA-RAY ABSORPTION COEFFICIENTS (D₂O REFLECTOR)
 (in cm⁻¹)

Material	Density, gm/cc	Gamma-ray Energy, mev				
		1	2.5	4	6	8
Core	-	0.1316	0.0779	0.0688	0.0660	0.0657
Heavy Water	0.8	0.0621	0.0392	0.0298	0.0244	0.0213
Steel	7.85	0.4694	0.3069	0.2591	0.2394	0.2339
Lead	11.3	0.7803	0.4823	0.4618	0.4940	0.5228
Concrete (Ord.)	2.4	0.1524	0.09696	0.07608	0.06432	0.05832
(Magnetite)	3.2	0.2032	0.1293	0.1014	0.0858	0.0778
(Magnetite & steel punchings)	4.26	0.2731	0.1737	0.1363	0.1152	0.1045

V. HEAT GENERATION

While it is not precise in nature, it is often sufficiently accurate to assume that all nuclear heating is caused by gamma rays that are absorbed, releasing their entire energy as heat at the point of absorption. A correction may be applied by using the energy absorption cross section rather than the total absorption cross section. Since this is rarely in error by as much as a factor of two, and is in the pessimistic direction, the total absorption cross section has been used for all the materials except the steel and lead.

It is necessary to make sure all sources of gamma rays have been included in determining the gamma-ray flux. In general, the most important source, outside of the fission process itself, is that produced by neutron absorption. This usually can be considered predominantly resulting from thermal neutron captures. It is well, however, to estimate heating due to fast neutron scattering, both elastic and inelastic, as well as fast neutron absorption. An order of magnitude estimate can be made quite rapidly to eliminate doubts.

A formula that expresses the heat generation, once the gamma-ray flux has been determined, is

$$H = \sigma E \Phi_{\gamma} \text{ mev/cm}^3 \text{ sec}, \quad (17)$$

where

σ = gamma-ray energy absorption coefficient (cm^{-1}),

E = gamma-ray energy (mev),

Φ_{γ} = gamma-ray flux ($\gamma/\text{cm}^2 \text{ sec}$).

While this is quite a naïve approach it must be remembered that the heating cannot be more accurately determined than the gamma-ray flux. In addition, the longer period of time spent in a more accurate analysis may cost more than the accuracy warrants.

The heat generation for the EBWR shield has been determined on the basis of the preceding discussion. The results for the light water-moderated design are plotted in Fig. 20. The results for the heavy water-moderated version are plotted in Fig. 21.

ACKNOWLEDGEMENT

It is a distinct pleasure to acknowledge the generous contribution of effort to this project by R. J. Rickert. The authors also wish to gratefully acknowledge the calculations performed by A. E. McCarthy, A. D. Rossin, C. K. Soppet, S. A. Bernsen, M. G. Schlapkohl, and J. J. Mikulski.

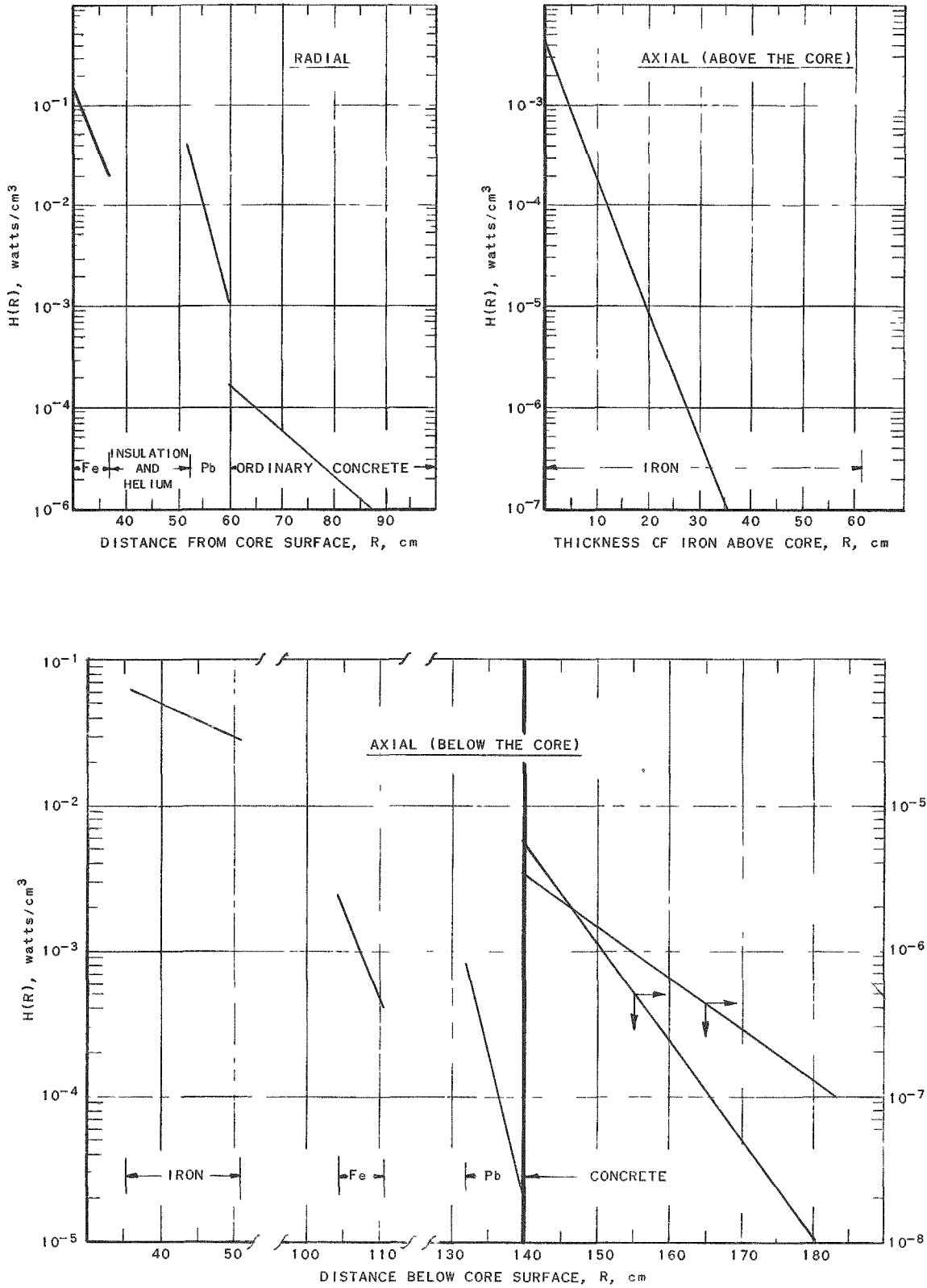


FIG. 20
 CALCULATED HEAT GENERATION IN THE EBWR SHIELD (H_2O REFLECTOR)

2/1

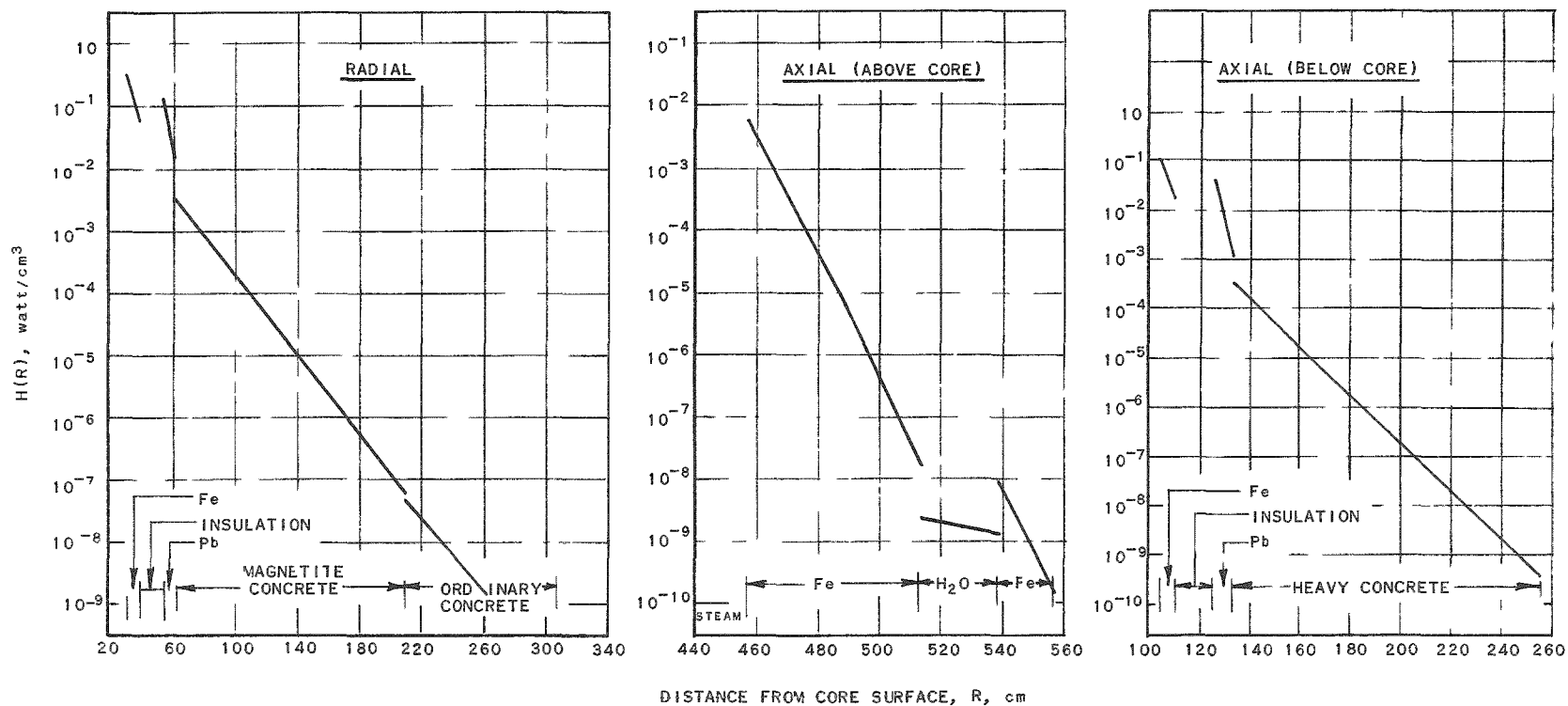


FIG. 21
CALCULATED HEAT GENERATION IN THE EBWR (D_2O REFLECTOR)

RE-7-18653-B

BIBLIOGRAPHY

1. Reactor Engineering Division Quarterly Report, ANL-5297 (June 30, 1954) p. 56.
2. Ibid, ANL-5461 (March 31, 1955) p. 69.
3. Ibid, ANL-5511 (September 30, 1955) p. 39.
4. Ibid, ANL-5561 (December 31, 1955) p. 48.
5. R. D. Albert, T. A. Welton, "A Simplified Theory of Neutron Attenuation and Its Application to Reactor Shield Design," WAPD-15 (November 30, 1950).
6. T. Rockwell (Editor), Reactor Shielding Design Manual, TID-7004 (March, 1956) pp. 6, 48.
7. Ibid, pp. 7, 71.
8. Ibid, p. 52.
9. Ibid, p. 372.
10. Ibid, p. 380.
11. Ibid, pp. 34, 39.
12. E. P. Blizzard, "Nuclear Radiation Shielding," Annual Review of Nuclear Science, (Annual Reviews Inc. Stanford, Calif.) 5, 73 (1955)
13. A. Simon, "Neutron Attenuation," Reactor Handbook, AECU-3645 (March, 1955), Vol. 1 (Physics), pp. 671-675.
14. C. E. Clifford, "The ORNL Shield Testing Facility," ORNL-402 (November 4, 1949).
15. G. Placzek, "The Functions $E_n(x)$," MT-1, (Ottawa, Canada: National Research Council of Canada #1547).
16. J. LeCaine, "A Table of Integrals Involving the Functions $E_n(x)$," MT-131, (Ottawa, Canada: National Research Council of Canada #1553).
17. "Tables of Sine, Cosine, and Exponential Integrals," Federal Works Agency, Works Project Administration for the City of New York (1940) Vols. I and II.
18. "Project Handbook," CL-697, Chap. V.
19. P. Mittleman, "Gamma-Rays Resulting From Thermal Neutron Capture," NDA-10-99 (October 6, 1953). [Nucleonics 13, (1955), p. 50].
20. G. R. White, "X-Ray Attenuation Coefficients From 10 kev to 100 mev," NBS-1003 (May 13, 1952).